Heslop, J., Walter Anthony, K. M., Winkel, M., Sepulveda-Jauregui, A., Martinez-Cruz, K., Bondurant, A., Grosse, G., Liebner, S. (2020): A synthesis of methane dynamics in thermokarst lake environments. - Earth-Science Reviews, 210, 103365.

https://doi.org/10.1016/j.earscirev.2020.103365

A synthesis of methane dynamics in thermokarst lake environments

Heslop, J.K.[1], Walter Anthony, K.M.[2,3], Winkel, M.[4], Sepulveda-Jauregui, A.[5], Martinez-Cruz, K.[5], Bondurant, A.[2], Grosse, G.[6,7], and Liebner, S.[1,8]

[1] GFZ German Research Centre for Geosciences, Section 3.7 Geomicrobiology, Helmholtz Centre Potsdam, Potsdam, Germany
[2] Water and Environmental Research Center, University of Alaska Fairbanks, Fairbanks, Alaska, USA
[3]International Arctic Research Center, University of Alaska Fairbanks, Fairbanks, AK, USA
[4] GFZ German Research Centre for Geosciences, Section 3.5 Interface Geochemistry, Helmholtz Centre Potsdam, Potsdam, Germany
[5] Environmental Biogeochemistry in Extreme Ecosystems Laboratory (EnBEELab), University of Magallanes, Punta Arenas, Chile
[6] Alfred Wegener Institute Helmholtz Centre for Polar and Marine Research, Potsdam, Germany
[7] University of Potsdam, Institute of Geosciences, Potsdam, Germany
[8] University of Potsdam, Institute of Biochemistry and Biology, Potsdam, Germany

Abstract

Greenhouse gas emissions from physical permafrost thaw disturbance and subsidence, including the formation and expansion of thermokarst (thaw) lakes, may double the magnitude of the permafrost carbon feedback this century. These processes are not accounted for in current global climate models. Thermokarst lakes, in particular, have been shown to be hotspots for emissions of methane (CH_4), a potent greenhouse gas with 32 times more global warming potential than carbon dioxide (CO_2) over a 100-year timescale. Here, we synthesize several studies examining CH_4 dynamics in a representative first-generation thermokarst lake (Vault Lake, informal name) to show that CH_4 production and oxidation potentials vary with depth in thawed sediments beneath the lake. This variation leads to depth-dependent differences in both *in situ* dissolved CO_2:CH_4 ratios and net CH_4 production responses to additional warming. Comparing CH_4 production, oxidation, and flux values from studies at Vault Lake suggests up to 99% of produced CH_4 is oxidized and/or periodically entrapped before entering the atmosphere. We summarize these findings in the context of CH_4 literature from thermokarst lakes and identify future research directions for incorporating thermokarst lake CH_4 dynamics into estimates of the permafrost carbon feedback.

Keywords

methane, methane oxidation, permafrost carbon feedback, rapid thaw

1. Introduction

The Arctic is currently experiencing a geologically abrupt climate warming event where major portions have warmed by more than 1 °C per decade during the past 40 years (Jansen et al., 2020). Temperatures in the Arctic are anticipated to increase a further 4-7 °C during the 21st century (Post et al., 2019). Permafrost regions, which represent around a quarter of the Arctic, are estimated to contain almost 1700 Pg of soil organic carbon (SOC) (Schuur et al., 2015), making them a globally important carbon (C) stock. Permafrost warming and thaw, triggered by climate warming, is expected to mobilize ~288 Pg of permafrost SOC by 2300 (Turetsky et al., 2020). A portion of this mobilized permafrost C will be microbially mineralized into the greenhouse gasses (GHG) methane (CH_4), carbon dioxide (CO_2), and nitrous oxide (N_2O), which will contribute a positive feedback to climate warming called the permafrost carbon feedback (PCF) and potentially turn the Arctic to a net C source to the atmosphere (Schuur et al., 2015; Voigt et al., 2020). Estimates of the PCF suggest that C released from thawing permafrost can increase global climate warming by 0.13-0.27 °C by 2100 (Schuur et al., 2015). However, these models are based on gradual, top-down permafrost thaw (e.g. active layer deepening). The impact of comparatively rapid physical disturbance thaw processes (e.g. thermokarst and coastal erosion) are not accounted for in current estimates of the PCF (Tanski et al., 2019; Turetsky et al., 2019, 2020).

In the Arctic, lakes have been identified as hotspots where terrestrial C, including C from thawed permafrost, is mineralized and emitted as CH_4 and CO_2 (Kuhn et al., 2018; Walter et al., 2006; Wik et al., 2016). Lakes are a common feature in northern latitudes; by surface area, almost half of the world's lakes are located in Arctic and sub-Arctic regions (Smith et al., 2007; Grosse et al., 2013). Thermokarst (thaw) lake landscapes are widespread in permafrost-underlain regions and cover 1.3 million km^2, representing 20-40% of the permafrost region and 15-75% of arctic lowland surface area (Olefeldt et al 2016). These lakes usually form when ice-rich permafrost thaws or massive ice melts (thermokarst) in areas with low relief, thick unconsolidated sediments, and high ground ice contents (Jones et al., 2011); the formation of this type of lake is expected to become more widespread with climate change (Grosse et al., 2013; Jones et al., 2011). Once formed, thermokarst lake expansion can rapidly introduce new C into the active C cycle. Talik (thaw bulb) development beneath the lake can thaw and mobilize older, deeper C that otherwise would not thaw during this century, even under the most severe active layer deepening scenarios (Langer et al., 2016; Walter Anthony et al., 2018).

Thermokarst lakes currently contribute almost a quarter (4.1± 2.2 Tg CH_4 yr^{-1}; Wik et al., 2016) of the total CH_4 emitted annually from northern lakes. CH_4 and CO_2 emissions from thermokarst lakes are expected to increase five-fold during the coming century, and models suggest that accounting for GHG produced in and released from thermokarst lakes will more than double the PCF this century (Schneider von Deimling et al., 2015; Walter Anthony et al., 2018). Much of the C used to produce GHG originates from the surrounding terrestrial environment, including reworked eroded and deposited sediments and permafrost thawing beneath the lake. Carbon mass balance measurements of paleo thermokarst lake taliks by Walter Anthony et al. (2014) suggest 28 ± 12% of thawed C beneath thermokarst lakes is converted to GHG over the lakes' millennial-scale lifespans. Additional, modern C can be contributed by primary productivity and vegetation within and surrounding the lakes (Dean et al., 2020; Elder et al., 2018).

Understanding CH_4 emissions from thermokarst lakes is particularly important given that CH_4 has 96x more global warming potential (GWP) than CO_2 over a 20-year timescale and 32x more GWP than CO_2 over a 100-year timescale (Alvarez et al., 2018; Etminan et al., 2016). One approach towards constraining estimates of CH_4 emissions in these rapidly changing landscapes is examining CH_4 emission, production, and oxidation dynamics in thermokarst lake environments. Here, we synthesize research conducted on CH_4 dynamics at a thermokarst lake in central Alaska to provide insights into whole-lake CH_4 cycling in a thermokarst lake system and the role CH_4 emissions from thermokarst lakes may play in the PCF. To our best knowledge, this is the most detailed biogeochemical and microbiological study of a sediment core capturing the full depth profile of a thermokarst lake talik. We used sediment from a lake core collected from the center of Vault Lake (informal name) and extending through the entire talik to examine: (1) CH_4 production potentials (Heslop et al., 2015); (2) aerobic (Martinez-Cruz et al., 2015) and anaerobic (Martinez-Cruz et al., 2017; Winkel et al., 2019) CH_4 oxidization; (3) temperature sensitivities of CH_4 production (Heslop et al., 2019a); and (4) CH_4-producing and oxidizing microbial communities (Heslop et al., 2019a; Martinez-Cruz et al., 2018; Winkel et al., 2019). We also measured *in situ* sediment CH_4 concentrations (Winkel et al., 2019) and the whole-lake CH_4 emission budget (Sepulveda-Jauregui et al., 2015) at the same lake for comparison with results from our laboratory studies. Our examination provides unique and valuable insights on C cycling dynamics in thawed sediments beneath thermokarst lakes. Further, we draw upon research from lakes in other northern and global environments to fill knowledge gaps in CH_4 dynamics not studied at Vault Lake, to place our findings in a global context, and to identify future research directions for incorporating thermokarst lake CH_4 dynamics into estimates of the PCF.

2. Study site: Vault Lake

Lake location and characteristics

Vault Lake (65.0293 °N, 147.6987 °W, elevation 216 m) is a 3,200 m^2 thermokarst lake located in a lowland boreal region of Interior Alaska approximately 40 km north of Fairbanks. The region has a continental climate (mean annual air temperature -2.39 °C and 274.6 mm mean annual precipitation; 1981-2010 data from the National Climate Data Center) and is characterized by discontinuous permafrost reaching up to 120-m thick (Jorgenson et al., 2008). At the Vault site, permafrost is comprised of 36-m thick ice- (21-208 wt% gravimetric ice content with ice wedges up to 3 m width) and organic-rich (1-3 wt% SOC) aggraded syngenetic loess-like silt (yedoma) underlain by schistose bedrock. These yedoma sediments were largely deposited in the unglaciated region during the early and middle Wisconsin periods, and observed ice wedge and sediment deformation suggests displacement (e.g. from landslides) following permafrost formation (Schirrmeister et al., 2016). Similar ice- and organic-rich yedoma deposits are found in unglaciated lowland regions across Alaska, Northeast Siberia, and Northwest Canada (Olefeldt et al., 2016; Walter Anthony et al. 2018).

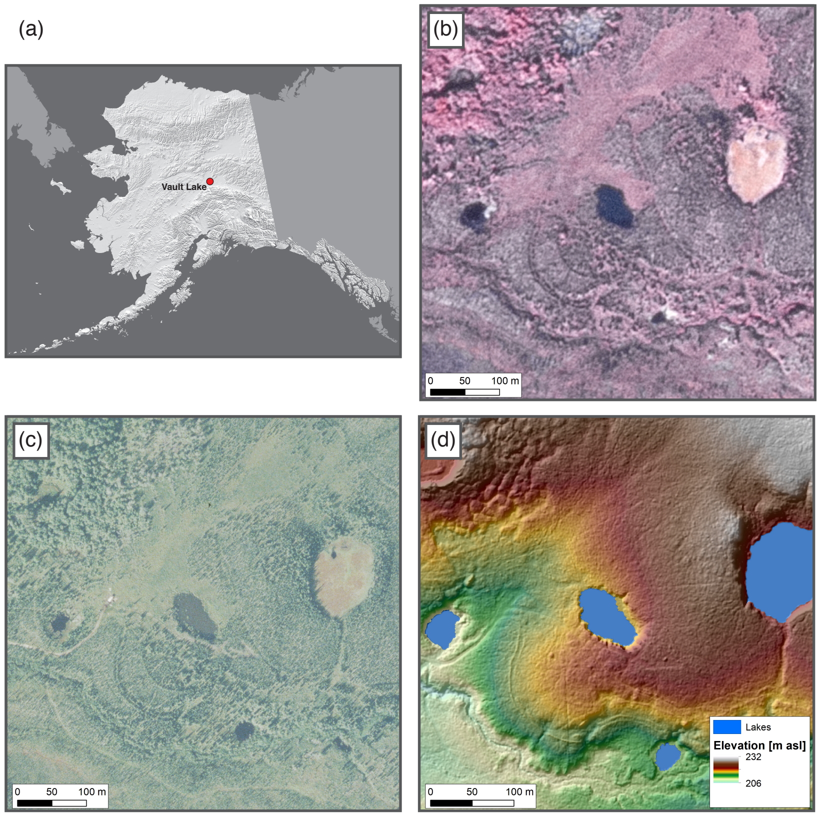

Figure 1. Location map of Vault Lake (a) and historical and recent georeferenced aerial images and LiDAR digital elevation model of the Vault Lake study area: (b) false color near-infrared aerial photo from 22 August 1986 from the Alaska High-Altitude Aerial Photography (AHAP) program; (c) true color aerial photo from 18 August 2007 from the USGS Digital Orthophoto Quadrangle (DOQQ) program for Alaska; and (d) LiDAR-based digital elevation model of the same study area from May 2011 produced by the Alaska Division of Geological and Geophysical Surveys (DGGS).

Vault Lake is representative of a young thermokarst lake in a yedoma permafrost setting. We note that not all thermokarst lakes are located in yedoma-type permafrost and, compared to thermokarst lakes formed in non-yedoma environments, thermokarst lakes in yedoma permafrost are typically deeper due to higher ground subsidence from melting massive ice (Grosse et al., 2013). Vault Lake has an average water depth of 3.7 m (maximum depth 4.6 m; Heslop et al., 2015) and reached a maximum lake ice thickness of 60-80 cm in late winter during 2012-2014 (Bondurant, *unpublished data*). Temperature and dissolved oxygen profiles measured in the water column during February-June 2013 indicate Vault Lake stratifies at 1.0-1.5 m depth (Fig.

2), leading to an anoxic hypolimnion and talik. Talik depths, measured in a 2013 borehole transect, range from 5.5 to 8.8 m (Heslop et al., 2015). For comparison, other Fairbanks-region thermokarst lake taliks measured via boreholes (Walter Anthony et al., 2018; Walter Anthony et al., *submitted*; Winkel, *unpublished data)* and nuclear magnetic resonance (Parsekian et al., 2013) range from 5 to 22 m depth. No evidence of prior drained thermokarst lakes at the site indicate Vault Lake is thawing into the yedoma for the first time and, therefore, is a first-generation lake. Steep eroding bluffs along the lake margin are a sign of active lateral lake expansion and numerous active ebullition seeps emitting CH_4 with a ^{14}C-depleted signature characteristic of Pleistocene-aged substrates (^{14}C-CH_4 age up to 28,500 ±140 yrs BP; δD -383 to -413‰; Winkel et al., 2019) indicate the talik is still deepening and thawing the underlying yedoma permafrost. Silt mobilized from soils in the lake's watershed is carried into the lake during rain events via overland flow, with mud flows moving over the top of the organic horizon, between tussocks and other types of vegetation. In addition to shore erosion, these mudflows contribute to the accumulation of organic-rich (3.83 ± 1.66 wt% SOC; Heslop et al., 2015) mineral sediments in the lake at an estimated rate of 0.2 to 0.8 cm yr^{-1} (Bondurant, *unpublished data*).

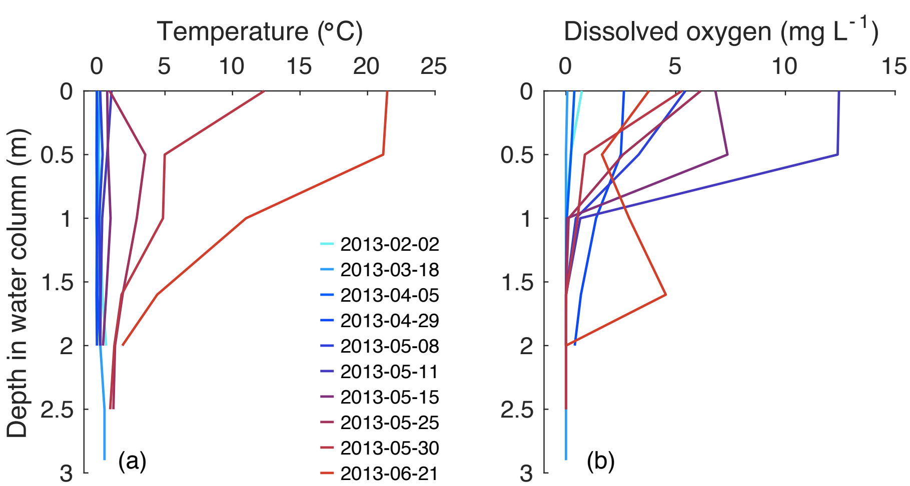

Figure 2. Water column temperature (a) and dissolved oxygen (b) profiles measured at Vault Lake during February-June 2013. The data suggest Vault Lake stratifies at 1.0-1.5 m depth and show the hypolimnion is anoxic.

Sediment core

In March 2013, we collected a 590-cm long sediment core from the center of Vault Lake. Core drilling, processing, and storage methods are described in detail in Heslop et al. (2015). The Vault Lake core captured the near-complete deposited lake sediment and thawed talik sediment sequence beneath the lake, in addition to the top 40 cm of permafrost beneath the talik. Sediment characteristics (Heslop et al., 2015) and organic matter composition (Heslop et al., 2017) were used to classify the core into five facies: (1) Organic-rich mud (0-152 cm); (2) Lacustrine silt (152-330 cm); (3) Taberite (330-508 cm); (4) Recently thawed taberite (508-550 cm); and (5) Transitional permafrost (550-590 cm). The Organic-rich mud (mean 3.83 wt% SOC; 1.86 wt% IC) and Lacustrine silt (1.04 wt% SOC; 0.56 wt% IC) facies represent terrestrial sediments deposited following the lake formation that were exposed to the lake water column during erosion and re-deposition (Heslop et al., 2015). Taberite (0.84 wt% SOC; 0.38 wt% IC) represents yedoma sediment which thawed *in situ* and remained underneath the lake (Walter Anthony et al., 2014; Schirrmeister et al., 2011); the bottom 43 cm of the taberite, representing the most recently thawed sediments, was designated as Recently-thawed taberite (1.36 wt% SOC; 0.70 wt% IC). The Transitional permafrost (1.52 wt% SOC; 0.88 wt% IC) facies consisted of permafrost beneath the talik thaw front that was frozen at the time of core collection; we refer to this as "transitional permafrost" because it is close to the thaw transition and therefore contains a large amount of unfrozen water in the inter-pore space (Williams and Smith, 1989).

Lake age

We estimate Vault Lake formed 100-400 years before present (yr BP). Using AMS radiocarbon ages of macrofossils picked from the Vault Lake sediment core, we had originally estimated the lake age to be around 400 yr BP (Heslop et al., 2015). However, estimating the date of lake formation using expansion rates between 1951 and 2007 shorelines (Fig. 3) yields a lake age estimate of 100 yr BP. Using the depth of the deposited Organic-rich mud (0-152 cm) facies and assuming a sediment deposition rate of 0.2 to 0.8 cm yr^{-1} yields lake age estimates of 190-760 yr BP. The variance in lake age estimates obtained using different methods highlights the challenges of accurately dating thermokarst lake initiation. Using AMS radiocarbon ages of macrofossils has the potential to overestimate lake age if pre-aged materials enter the sediment column. Similarly, lake expansion and sediment disposition rates are unlikely to be constant over the lakes' history, which can lead to over- or underestimating lake age. These challenges to accurately estimating thermokarst lake age point towards the difficulties of modeling and projecting CH_4 emissions from thermokarst lakes in the coming centuries, given that younger thermokarst lakes typically have higher CH_4 emission rates than older thermokarst lakes (Turetsky et al., 2020; Walter Anthony et al., 2018).

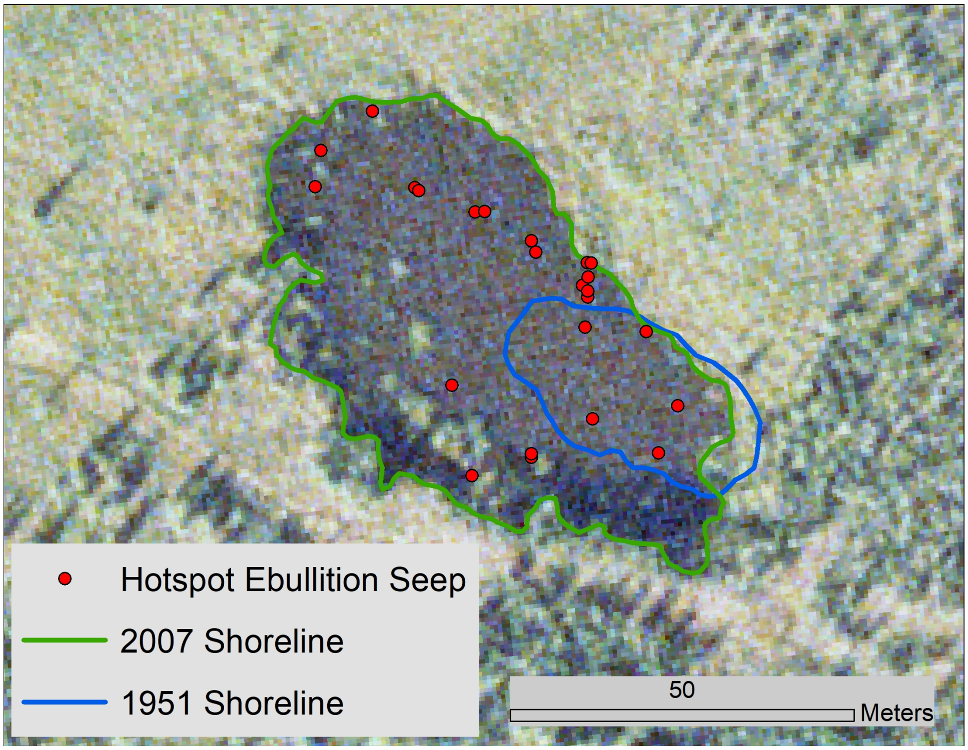

Figure 3. Locations of hotspot ebullition seeps (red) mapped at Vault Lake during October 2014 in relation to the 2007 shoreline (green) and 1951 shoreline (blue).

Talik temperatures

Temperatures measured in two vertical profiles within the talik over a seven-year period (2013-2020; Fig. 4) indicate sediments in the lake center (4.0 m water depth) range from -0.40 to 4.51 °C (annual mean ± SD 1.11 ± 1.42 °C) and sediments near the lake margin (1.4 m water depth) range from -0.40 to 14.45 °C (annual mean ± SD 2.50 ± 3.37 °C). Temperatures at all depths in both talik profiles were significantly correlated with atmospheric temperatures. Temperatures from the shallower sediment depths (0.5 and 1.0 m) in the profile near the lake margin were positively correlated with atmospheric temperatures (Pearson coefficient $r = 0.59$ and 0.44, respectively; $p < 0.001$), while temperatures in the same sediment depths in the lake center were negatively correlated with atmospheric temperatures (Pearson coefficient $r = -0.34$ and -0.52 ; $p < 0.001$). This is most likely a result of: (1) the deeper water in the lake center causing less efficient heat transfer from the atmosphere to the sediments, resulting in a lagged temperature response compared to the sediments in the lake margin profile, and (2) water beneath the hypolimnion in the lake center remaining colder during the thaw season than water in the shallower littoral zones.

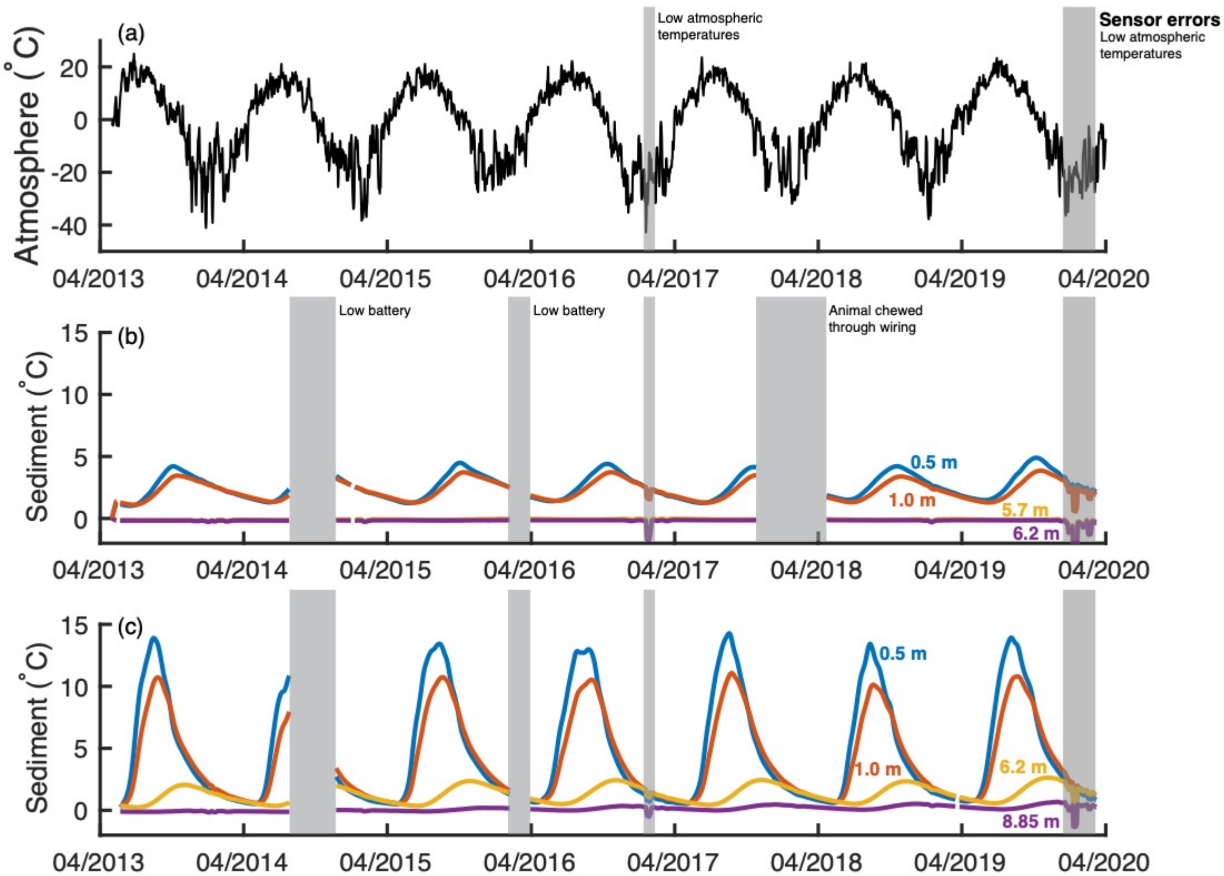

Figure 4. Mean daily atmospheric temperatures measured at Fairbanks, Alaska (a; data from ACIS) and hourly temperatures measured at the Vault Lake talik in the lake center (b; 4.0 m water depth) and near the lake margin (c; 1.4 m water depth). Temperature data were recorded continuously, except for gaps and sensor errors noted in gray on the figure.

3. Methane emission

High latitude lakes emit CH_4 by four main seasonal pathways: diffusion, direct ebullition, ice bubble storage flux, and storage flux turnover events (Greene et al. 2014). Atmospheric diffusion occurs during ice-free conditions when the lake water becomes oversaturated in CH_4, leading to positive diffusive flux to the atmosphere. Diffusive CH_4 flux is the lowest contribution of CH_4 to the atmosphere, contributing approximately 5% of total annual emissions from interior Alaska yedoma lakes (Sepulveda-Jauregui et al., 2015). Ebullition is the dominant pathway of CH_4 emission in most thermokarst lakes (Walter et al., 2006). Direct ebullition occurs when high concentrations of CH_4, which is less soluble than CO_2, accumulate in sediment pore space. When concentrations exceed the solubility limits, free gas bubbles form. Bubbles form and migrate through secondary pore channels in sediments to release gas to the atmosphere (Liu et al., 2016; Scandella et al., 2011), with the highest ebullition rates occurring when hydrostatic pressure drops (Varadharajan, 2009). In winter surface lake ice impedes bubble release to the atmosphere, entrapping many CH_4 ebullition bubbles in and under surface lake ice. Up to 80% of their CH_4 content may be lost to the water column when CH_4 diffuses out of bubbles before the ice thickens around them. When the ice melts in spring, the remaining entrapped CH_4 is released to the atmosphere through a process called ice bubble storage flux (Greene et al., 2014). Combined, ebullition and ice bubble storage flux typically account for around 86% of annual CH_4 emissions from thermokarst lakes formed in yedoma-type permafrost (Sepulveda-Jauregui et al., 2015). Elevated concentrations of dissolved CH_4 in the water column beneath ice are also subject to diffusive flux as the ice melts and during overflow events (Greene et al., 2014). These emissions associated with springtime storage flux turnover events, which derives largely from dissolution of ebullition bubbles beneath ice in winter (Greene et al., 2014), contributes 1.2% of total annual CH_4 emissions (Sepulveda-Jauregui et al., 2015).

At Vault Lake, total annual CH_4 emissions were estimated to be 40.9 g CH_4 m^{-2} yr^{-1}; 77% of the annual CH_4 flux is from ebullition, 11% is from ice bubble storage flux, and 12% is from diffusive flux (Sepulveda-Jauregui et al., 2015). Diffusive flux and ice bubble storage flux values at Vault Lake are near the median for the yedoma lakes, while ebullitive flux is slightly higher than the median but still within the interquartile range for yedoma lakes (Fig. 5). Compared to other reported CH_4 emissions values from northern lakes, net Vault Lake CH_4 emission values are near mean values for yedoma-type lakes (50.2 g CH_4 m^{-2} yr^{-1}; n = 13 lakes) and more than non-yedoma type lakes (mean 6.37 g CH_4 m^{-2} yr^{-1}; n = 36 lakes). This is consistent with prior research suggesting CH_4 emissions from thermokarst lakes in regions underlain by yedoma-type permafrost emit approximately 6x more CH_4 than lakes underlain by other permafrost types (Sepulveda-Jauregui et al., 2015). It is important to note that, as a relatively young thermokarst lake (100 - 400 yr BP), Vault Lake functions as a net C source to the atmosphere. As thermokarst lakes mature and eventually drain (typically over millennial time scales), their net C emissions become lower and, in some cases, negative due to C being sequestered in increased vegetative biomass (Walter Anthony et al., 2014). Emissions from newly formed thermokarst lakes (< 60 years old) are typically even higher than from older thermokarst lakes (Walter Anthony et al., 2018; Turetsky et al., 2020), such as Vault Lake. This variance in C emissions amongst thermokarst lakes highlights the importance of examining lakes in different environments to constrain their potential circum-arctic GHG emissions.

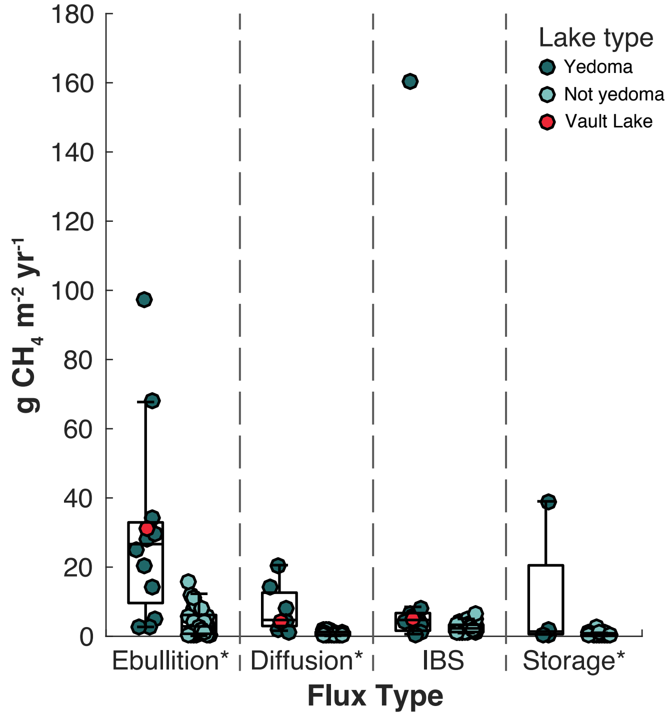

*Significant ($p < 0.05$) difference between yedoma and non-yedoma lakes

Figure 5. Magnitudes of CH_4 emission pathways from northern yedoma ($n = 13$) and non-yedoma ($n = 36$) lakes. IBS refers to ice bubble storage flux. Significant (Two-sample t test; $p < 0.05$) differences between yedoma and non-yedoma lakes are denoted. Emissions at Vault Lake, measured by Sepulveda-Jauregui et al. (2015), are highlighted in red. CH_4 flux values for diffusive flux and IBS at Vault Lake are near the median for the yedoma lakes, while ebullitive flux is slightly higher than the median, but still within the interquartile range. Spring storage flux following ice-out was not determined at Vault Lake. Data are reported by Huttunen et al. (2003), Repo et al. (2007), Sepulveda-Jauregui et al. (2015), Walter Anthony et al. (2010), and Zimov et al. (1997).

Within individual thermokarst lakes, CH_4 emissions vary spatially and temporally. However, most studies of northern lakes only report diffusive CH_4 emissions based on sampling < 1% of the lake surface area at 1-2 points in time (Engram et al., 2020). Further, the sporadic nature and spatial variability of ebullitive flux make it difficult to accurately estimate its magnitude. The bubble trap method, which is frequently used to measure ebullitive flux, is strongly biased as: (i) bubble traps are intentionally fixed over ebullition seeps; (ii) it is almost impossible to cover an stratified analysis for ebullition events due to variation in bottom topography, water depth, and sediment properties; (iii) the different number of traps installed in the ecosystems generates large uncertain in the literature reported; and (iv) the season and time measuring bubbles by traps varies between studies and sites (Wik et al., 2016). This variation makes it difficult to accurately quantify and compare CH_4 emissions from circum-arctic lakes. In addition to the lack of information on spatial and temporal variability, measurements of CH_4 emissions from lakes are scarce compared to the number of lakes. A 2016 synthesis by Wik et al. collected all known field measurements from northern lakes; the lakes studied (n = 733) represented only 0.02% of the 3.8 million lakes north of 50° N (Engram et al., 2020). This highlights the needs for additional data collection to constrain the spatial and temporal variability in CH_4 emissions from both thermokarst and non-thermokarst northern lake systems. Remote sensing methods have been suggested as one approach for constraining spatial and temporal variability in circum-arctic lake CH_4 emissions (Engram et al., 2020; Matthews et al., 2020).

While few field studies measure year-round temporal variability in CH_4 emissions, results from a process-based climate-sensitive lake biogeochemical model indicate that seasonal variation in CH_4 emissions can be explained by energy input and substrate availability (Tan et al., 2015). High temporal resolution CH_4 emissions have not been quantified at Vault Lake, but Sepulveda-Jauregui et al. (2015) determined annual summer CH_4 flux (ebullition and diffusive flux; 31.4 g CH_4 m^{-2} yr^{-1}) was approximately 3 times greater than annual winter CH_4 flux (ebullition and ice bubble storage; 9.4 g CH_4 m^{-2} yr^{-1}). Spatially, both field observations (Engram et al., 2020; Walter Anthony et al., 2016) and modeling results (Tan et al., 2015) show CH_4 emissions along the thermokarst margins are typically higher than emissions from non-thermokarst margins and centers in the same lake. Mapping of ebullition hotspots at Vault Lake during October 2014 suggest ebullition seep locations are generally more abundant in areas where the lake has expanded since 1951 (Fig. 3).

4. Methane production

Methane emissions from northern lakes originate from different sources, including fossil geological (microbial and thermogenic) sources and more recent microbial sources (Walter Anthony et al., 2012). Recently, in temperate lakes, CH_4 production in the water column has also been found to be associated with phytoplankton under oxic conditions (Günthel et al., 2020); however, it is currently unknown if oxic CH_4 production is also present in northern lakes. $\delta^{13}C$-CH_4 values collected from ebullition bubbles at Vault Lake (-67.7 ± 3.4‰; Winkel et al., 2019), in combination with Vault Lake having a closed talik without geologic CH_4 seeps, indicate CH_4 production at Vault Lake is microbial. Microbial production of CH_4 during anaerobic respiration, termed methanogenesis, occurs when *Archaea* called methanogens use simple substrate (CO_2, H_2, acetate, methyl compounds) to produce CH_4. Methanogenesis using CO_2 and H_2 as substrate, which is carried out by hydrogenotrophic methanogens (autotrophy), occurs when CO_2 is reduced to CH_4 according to the reaction:

$$CO_2 + 4H_2 \rightarrow CH_4 + 2H_2O \qquad \text{(Equation 1)}$$

Methanogenesis using acetate as a substrate (heterotrophy), carried out by acetoclastic methanogens, occurs when acetate is reduced to CH_4 according to the reaction:

$$C_2H_3O_2^- + H^+ \rightarrow CH_4 + CO_2 \qquad \text{(Equation 2)}$$

The primary pathway for CH_4 production (hydrogenotrophic vs. acetoclastic) varies both among yedoma thermokarst lakes and within the same lake depending on physiochemical parameters and substrate availability (Walter et al. 2008). At Vault Lake, a combination of archaeal sequencing measured from sediments and $\delta^{13}C$-CH_4 values measured from ebullition bubble gas indicates both hydrogenotrophic and acetoclastic methanogenesis by *Methanosarcina, Methanosaeta* and *Methanoregula* (Winkel et al., 2019). A less common pathway of methanogenesis that has been shown to be activated in thawing permafrost uses methyl compounds such as methylamines as a substrate (Canfield et al. 2005; Coolen and Orsi, 2015; Tveit et al., 2015). While we did not observe evidence of this CH_4 producing pathway at Vault Lake, incubations of thermokarst lake sediments from Utqiagvik, Alaska (de Jong et al., 2018) and Interior Alaska (Liebner, *unpublished data*) observed stimulation of methylotrophic methanogens following substrate addition.

Through an anaerobic incubation study of the Vault Lake sediment core, we found that two-thirds of total CH_4 measured during a 175-day incubation at 3 °C originated in the surface organic-rich mud facies (0-152 cm depth), despite this facies only representing a quarter of the core's total 590 cm thickness (Heslop et al., 2015). The organic-rich mud facies comprise of reworked allochthonous and autochthonous materials deposited since lake formation, as described by Farquharson et al. (2016) for other yedoma lakes. Archaeal communities were dominated (84% of detected sequences) by the acetoclastic methanogens *Methanosaetaceae*, with only a few hydrogenotrophic *Methanoregulaceae* and *Methanosarcinacae* (Heslop et al., 2019; Winkel et al., 2019). Given that all species within *Methanosaetaceae* only use acetate as substrate, their high abundance in the organic-rich mud facies suggests high availability of acetate. *Methanosaetaceae* and *Methanosarcinacae* are frequently detected methanogens in thermokarst lakes (Kallistova et al., 2020).

In an examination of bulk SOM composition using pyrolysis GC-MS, Heslop et al. (2017) found that the organic-rich mud facies had both greater substrate availability (higher C and N concentrations) and greater proportions of compounds associated with allochthonous terrestrial materials (alkanes, alkenes, lignin products, and phenols and phenolic precursors) compared to the underlying sediments. The abundance of these compounds was positively correlated with CH_4 production potentials measured in 3 °C incubations. Based on ^{14}C ages of picked macrofossils from the top 214 cm of the lake core (170 – 429 years BP; Heslop et al., 2015), the organic carbon (OC) in these deposited facies is far younger than in the Pleistocene-aged permafrost studied in the nearby Vault Creek Permafrost Tunnel (>20,000 years BP; Schirrmeister et al., 2016), which also underlies Vault Lake. Both ^{14}C ages of *in situ* dissolved C-CO_2 and C-CH_4 (Elder et al., 2018) and laboratory culture experiments (Douglas et al., 2020) suggest CH_4 is produced faster from younger C than older C in northern lakes. However, we note Elder et al. (2018) focused on the ^{14}C ages of dissolved C-CO_2 and C-CH_4, which escapes lakes by diffusion. In most arctic lakes, diffusion is a more minor component of total lake CH_4 emissions (~5% of total annual emissions; Sepulveda-Jauregui et al., 2015).

The radiocarbon age of CH_4 in naturally-emitted ebullition bubbles, which are the dominant form of CH_4 emissions in northern lakes (Bastviken et al., 2011; Sepulveda-Jauregui et al., 2015; Walter et al., 2006; Wik et al., 2016), is always ^{14}C-depleted and older than CH_4 dissolved in the water column (Walter Anthony et al., 2018). At Vault Lake, this was supported by the highest dissolved pore water CH_4 concentrations being at the talik thaw boundary, in the recently-thawed taberite facies (Winkel et al., 2019). The sediments directly above the thaw front also had high CH_4 production potentials in incubation studies of the Vault Lake core (Heslop et al., 2015), and above-median CH_4 ebullition rates observed at Vault Lake compared to other yedoma lakes (Fig. 4) suggest high CH_4 production rates and subsequent gas build up at the thaw front. The ^{14}C-CH_4 age (up to 28,500 ±140 yrs BP) and δD (-383 to -413‰) of ebullition bubbles emitted from Vault Lake reflect Pleistocene-yedoma carbon and hydrogen (from Pleistocene ice wedges) as the atomic components of the CH_4 molecules, as opposed to more modern (Holocene) sources which have younger/heavier CH_4 isotopic values (Brosius et al., 2012). This agrees with ebullition bubble mapping (Lindgren et al. 2016, 2019; Walter Anthony et al. 2016; Walter Anthony et al., *submitted*) and modeling studies (Kessler et al., 2012) of thermokarst lakes that suggest recently-thawed former permafrost at and directly above the thaw boundary is a source of high CH_4 production. The high CH_4 production at the thaw boundary may be due to high bioavailable substrate potential. The idea that permafrost dissolved OC (DOC) is more biodegradable than younger DOC is supported by a metanalysis showing higher observed DOC biodegradability with increasing permafrost landscape extent (Vonk et al., 2015). In terrestrial settings, DOC from recently thawed former permafrost has been shown to have higher degradation potentials than DOC from the overlying seasonally-thawed active layer (Heslop et al., 2019b; Liu et al., 2019; Selvam et al. 2017). Yedoma permafrost sediments have additionally been shown to have high acetate concentrations (Drake et al., 2015; Ewing et al., 2015), which can be directly utilized as substrate for acetoclastic methanogenesis following thaw. While acetate concentrations were not directly measured in the Vault Lake core, higher relative abundance of the acetoclastic methanogens *Methanosaeta* near the thaw front suggest higher acetate substrate potential. Like the organic-rich mud facies, archaeal communities in the recently-thawed taberite facies were dominated (89% of detected sequences) by the acetoclastic and hydrogenotrophic methanogens *Methanosaetaceae*, *Methanosarcinacae*, and *Methanoregulaceae* (Heslop et al., 2019a; Winkel et al., 2019).

Former permafrost sediments that have thawed *in situ* beneath Vault Lake over century timescales (152-508 cm core depth) had the lowest CH_4 production potentials indicated by both incubation studies (Heslop et al., 2015) and dissolved CH_4 concentrations (Winkel et al., 2019). The lacustrine silt and taberite facies, which represented 60% of the total Vault Lake core length, only accounted for 21% of the whole-column CH_4 production potential in the 3 °C incubation study (Heslop et al., 2015). Methanogens were only detected in the rare biosphere, which we defined as taxa below 0.1% relative sequence abundance of all detected archaea in our 16S RNA analyses. Detected methanogens included *Methanocellales*, *Methanoregulaceae*, *Methanosarcinacae*, and *Methanosaetaceae* (Heslop et al., 2019a; Winkel et al., 2019). Archaeal communities in this region were dominated by CH_4-consuming methanotrophs (see Section 5).

Using temperature sensitivity incubations, Heslop et al. (2019a) showed that these deeper, thawed *in situ* sediments had higher temperature sensitivities for CH_4 production compared to the overlying reworked and deposited material in the organic-rich mud facies. CH_4 production potentials did not increase with warming at incubation temperatures consistent with temperatures measured in the talik (0 °C and 3 °C) but increased with higher incubation temperatures (10 °C to 25 °C; Heslop et al., 2019a). This suggests CH_4 production in lacustrine silt and taberite facies is substrate-limited, and the input of additional energy with higher temperatures may increase CH_4 production potentials. In the lacustrine silt and taberite facies, we hypothesize the most labile "fast carbon pool" (days to years turnover time; < 5% of permafrost OC; Schädel et al., 2014) was previously exhausted. Per kinetic theory, the remaining, more complex OC (turnover times of decades to centuries) require higher activation energies for microbial decomposition due to the higher number of enzymatic steps needed for biological degradation (Davidson and Janssens, 2006, Conant et al., 2011). Hence, higher temperatures are needed to decompose the more recalcitrant sediment organic C. In contrast, the most deeply thawed sediments located at the talik boundary (i.e. the permafrost thaw front) showed the highest temperature sensitivity at a much lower temperature regime. The large increase in CH_4 production potentials when temperatures increased from 0 to 3 °C points to the higher bioavailability of the recently thawed, more labile permafrost organic C at the thaw front. We further discuss this in the context of changing climate in Section 7.

5. Methane oxidation

Methane production estimated from anaerobic laboratory incubations of the Vault Lake sediment core (2,819 g CH_4 m^{-2} at 3 °C ; Heslop et al., 2015) greatly exceeds the magnitude of CH_4 emitted annually by field flux measurements at the same lake (40.9 g CH_4 m^{-2}; Sepulveda-Jauregui et al., 2015). Using these values to calculate a first-order estimate suggests up to 99% of produced CH_4 at Vault Lake either accumulates and is held in sediments (presumably released during rare events not captured in field measurements) or is oxidized before being emitted to the atmosphere. A third possibility is that incubation conditions in closed vessels led to inflated CH_4 production potentials (i.e. the bottle effect; Ionescu et al., 2015) compared to actual CH_4 production, which is unknown; however, the 3 °C temperature of our incubation was slightly lower than the mean annual temperature of surface lake sediments (3.47 ± 3.07 °C at the 0.5 and 1.0 m depths), where most of the CH_4 was produced. This suggests that the actual rates in these surface lake sediments could be higher than our estimate. We acknowledge that our CH_4 production estimate does not take into account spatial and temporal heterogeneity affecting *in situ* CH_4 production and emissions at Vault Lake. Modelled CH_4 production at other Alaskan thermokarst lakes also indicate significantly more CH_4 is produced in sediments than is emitted into the atmosphere, with one study finding CH_4 production in a modeled thermokarst lake talik was up to 10 times higher than observed emissions in the field (Kessler et al., 2012).

Both globally and in the Arctic, CH_4 oxidation plays an important mitigating role in preventing a significant portion of CH_4 produced in lakes and wetlands from entering the atmosphere (Oh et al., 2020; Osudar et al., 2016; Reeburgh 2006). Calculations along the length of the Vault Lake core using stable isotopes suggest 41-83% of CH_4 produced in the core is anaerobically oxidized *in situ* (Winkel et al., 2019). Under anaerobic conditions, CH_4 oxidation often occurs as the result of syntrophic relationships between methanotrophic *Archaea* (ANME) and bacteria that reduce inorganic electron acceptors (Knittel and Boetius, 2009). However, recent research also showed that ANME can perform the process without a bacterial partner (Cai et al., 2018), the existence of anaerobic bacteria that internally produce oxygen to oxidize CH_4 (Ettwig et al., 2010), and that aerobic methanotrophs that can perform CH_4 oxidation under anaerobic conditions (Oswald et al., 2016). In the Vault Lake hypolimnion and sediments, which are under anoxic conditions year-round (Fig. 2b), anaerobic oxidation of methane (AOM) can occur using sulfate, nitrogen oxidizes, organic matter, chlorite, or metals (e.g. iron and manganese) as terminal electron acceptors. AOM values reported in the Vault Lake core by Winkel et al. (2019) ranged from 0 to 2.87 nmol CH_4 cm^{-3} d^{-1}. For comparison, reported AOM rates in global freshwater lake systems (n = 66) were 0.01 to 100 nmol CH_4 cm^{-3} d^{-1} (Martinez-Cruz et al., 2018). The lower values reported by Winkel et al. (2019) compared to global freshwater AOM rates are likely due to a combination of: (1) lower organic matter quality in the taberite facies, which had been thawed beneath Vault Lake for centuries, compared to in near-surface deposited sediments, which are where sediment AOM is typically quantified; and (2) the incubations conducted by Winkel et al. 2019 being done at 4 °C, which is a lower temperature than most of the incubations reported in literature.

To our knowledge, the study by Winkel et al. (2019) is the first to identify and quantify AOM in cold thawing and former permafrost sediments beneath a thermokarst lake. Tracer incubation studies of AOM potentials found low AOM potential rates in the transitional permafrost (~0.9 pmol cm^{-3} d^{-1}), but high (~660 μM) concentrations of nitrite (Winkel et al., 2019). Studies from another lake core collected in Interior Alaska suggest yedoma sediments also have high concentrations of Fe, which may serve as an alternate electron acceptor for AOM following thaw (Winkel, *unpublished data*). Evidence from the Vault Lake core suggests former permafrost sediments that have been thawed *in situ* for centuries (311 to 532 cm depth; taberite and recently-thawed taberite facies) are a region of high AOM in thermokarst lake environments. Compared to the transitional permafrost, AOM rates doubled in the overlying recently-thawed taberite facies. This region of the Vault Lake core had the highest AOM potential rates (up to 2.88 pmol cm^{-3} d^{-1}; mean 1.7 ± 0.7 pmol cm^{-3} d^{-1}), high nitrite concentrations, and the most fractionated $\delta^{13}C$-CH_4 in the pore waters (Winkel et al., 2019). Archaea in this region were almost exclusively the nitrate-driven AOM (Haroon et al 2013) or iron-driven AOM (Ettwig et al 2015, Cai et al 2018) archaea *Methanoperedenaceae* (Winkel et al., 2019). Sulfate concentrations in the taberite (up to 35 ± 2 mM) were also found to be sufficient for potentially supporting AOM (Winkel et al., 2019).

A second region of high AOM was observed in the deposited near-surface sediments of Vault Lake. Winkel et al. (2019) found the top 100 cm of the Vault Lake core to have high AOM potential rates (up to 2.3 pmol cm^{-3} d^{-1} at 3 °C). Mean AOM potential rates separately measured by Martinez-Cruz et al. (2017) in sediments collected from the top 25 cm were 12.27 ± 3.96 nmol cm^{-3} d^{-1} (mean ± SD) at 4 °C. Compared to net CH_4 production potential rates measured from the same 25 cm core at the same incubation temperature, this represents approximately one-third of CH_4 produced in surface sediments at Vault Lake being anaerobically oxidized (Martinez-Cruz et al., 2017). AOM in this region used different electron acceptors and had different methanotrophs compared to the high AOM in the underlying taberite. This AOM was mainly attributed to type I aerobic methanotrophs belonging to the genus *Methylobacter*; only iron and manganese were found to be present in sufficient quantities to support the observed AOM (Martinez-Cruz et al., 2017).

Synthesizing published rates of CH_4 oxidation from Alaskan yedoma (n = 38 observations) and non-yedoma (n = 53 observations) lakes revealed that lakes located in yedoma regions did not have significantly different oxidation rates (aerobic or anaerobic) in their sediment than non-yedoma northern lakes (Fig. 6). While we did not examine CH_4 oxidation in the water column at Vault Lake, research from nearby Alaskan thermokarst lakes and other arctic lakes suggests further CH_4 oxidation occurs in the water column and under ice under both aerobic and anaerobic conditions. A study by Martinez-Cruz et al. (2015) in yedoma-type lakes near Vault Lake found mean potential aerobic CH_4 oxidation rates of 0.71 mg L^{-1} d^{-1} in the summer and 0.18 mg L^{-1} d^{-1} in the winter. Our literature synthesis suggests median potential CH_4 oxidation rates in the water columns of yedoma lakes are higher than in non-yedoma lakes (Fig. 6). A recent study by Thalasso et al. (2020) found that, in a stratified lake in north-central Siberia, all CH_4 produced in the sediments and deep hypolimnion was removed below the oxycline, suggestive of high AOM. This case study suggests, in northern lakes that stratify, it is possible for most or all CH_4 produced in sediments to be anaerobically oxidized in the hypolimnion, resulting in little to no CH_4 exchange with the epilimnion and/or atmosphere. In northern Alaska, it has been suggested that the threshold depth for lakes to fully stratify is approximately 4 m (Arp et al., 2015). At Goldstream Lake, a thermokarst lake located in interior Alaska, approximately 50% of CH_4 in ebullition bubbles trapped under winter ice cover oxidize prior to ice out (Elder et al., 2019). Greene et al. (2014) estimated the under-ice CH_4 oxidation at the same lake to be 56%. ^{13}C-CH_4 analyses of ice cores from thermokarst lake and lagoon environments underlain by continuous permafrost in Siberia revealed that CH_4 at the ice-water interface was oxidized to concentrations near atmospheric equilibrium, while the overlying ice was supersaturated in CH_4 compared to atmospheric concentrations (Spangenberg et al., *in review*).

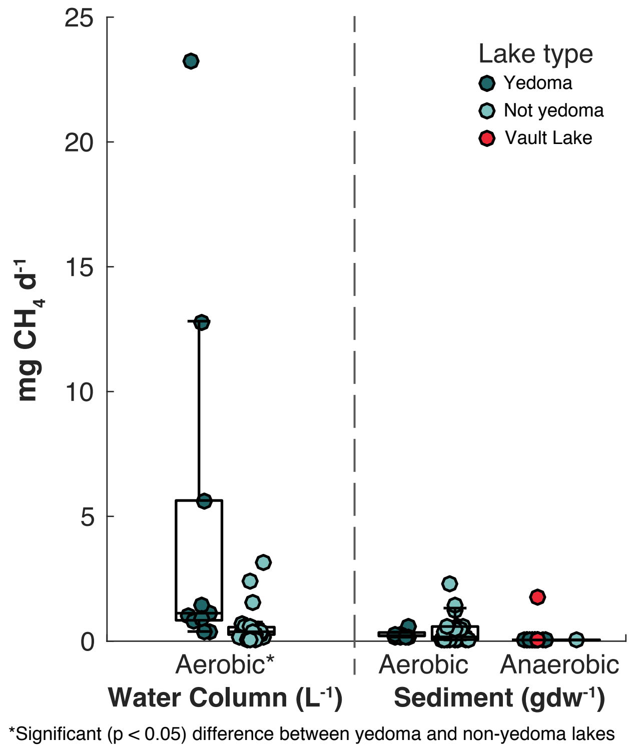

Figure 6. Rates of CH_4 oxidation from Alaskan yedoma (n = 38 observations) and non-yedoma (n = 53 observations) lakes. Significant (two-sample t-test; $p < 0.05$) differences between yedoma and non-yedoma lakes are denoted. Sediment AOM at Vault Lake, measured by Martinez-Cruz et al. (2017) and Winkel et al. (2019), are highlighted in red. Data are reported by de Jong et al. (2018), He et al. (2012), Martinez-Cruz et al. (2015, 2017), Miller et al. (2019), and Winkel et al. (2019).

6. Carbon dioxide to methane production ratios

One issue of great importance in determining the potential impact of C emissions from thermokarst lakes on the global C cycle is determining proportions of C released as CO_2 versus CH_4. Northern lakes emit more CO_2 than CH_4; on average 26x more CO_2 was emitted than CH_4 in a transect of 40 lakes in Alaska (Fig. 7; Sepulveda-Jauregui et al., 2015). Several processes in both the lake sediments and overlying water column affect the magnitudes of CO_2 versus CH_4

emissions. Analysis of data from 5,118 boreal lakes found that CO_2 emissions were predominately (60% of studied lakes) sustained by loading from the catchment (e.g. inorganic C loading from surface and ground waters), as opposed to internal CO_2 production (Weyhenmeyer et al., 2015). In the aerobic portion of the water and sediment column, internal processes that produce CO_2 include: biological respiration in the water column (3.4–91% of internal CO_2 production in boreal lakes; Weyhenmeyer et al., 2015) and sediments (4.0-60% internal CO_2 production); inorganic C fixation; and, in shallow non-yedoma lakes (Tan et al., 2017), light degradation (3.0-48% internal CO_2 production). In anaerobic portions of the water column and in lake sediments, CO_2 is produced both as a by-product of methanogenesis and fermentation, and as an end-product of CH_4 oxidation; CH_4 is produced as an end-product of methanogenesis. In both the sediments and water column, under both aerobic and anaerobic conditions, a significant amount of CH_4 is removed and CO_2 is produced during CH_4 oxidation.

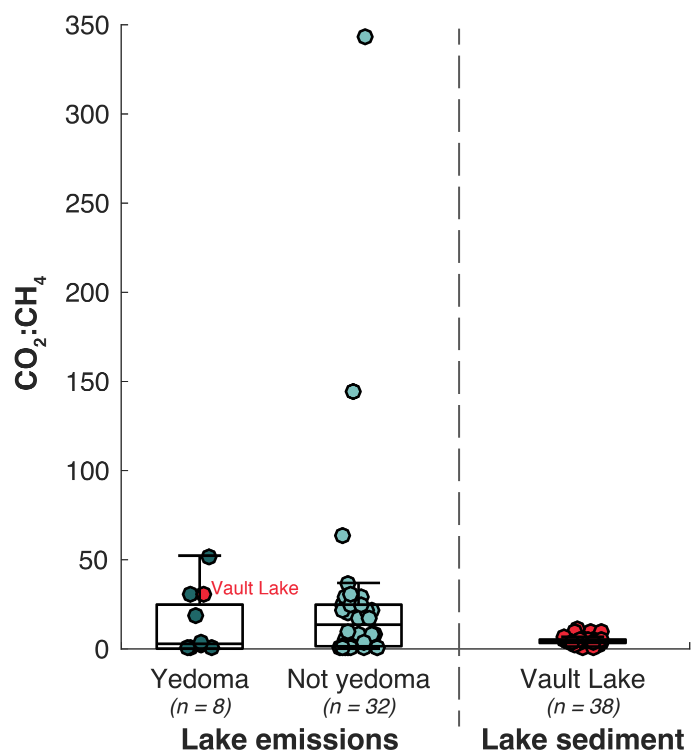

Figure 7. *In situ* ratios of CO_2:CH_4 emissions measured in Alaskan lakes vs. CO_2:CH_4 porewater concentrations in Vault Lake sediments. Annual CO_2 and CH_4 emissions were reported by Sepulveda-Jauregui et al. (2015). Emission CO_2:CH_4 ratios were not significantly different in yedoma versus non-yedoma lakes (two-sample t-test; $p = 0.51$). Pore water dissolved gas concentrations in anaerobic lake sediment, measured in the Vault Lake core, were reported by Winkel et al. (2019).

It had been previously thought that, under stable anaerobic CH_4-producing conditions, the lowest possible ratio of CO_2:CH_4 production is 1:1 (Conrad, 1999). However, some recent studies from Arctic environments have reported CO_2:CH_4 ratios of less than 1, indicating more CH_4 production than CO_2 production (Heslop et al., 2019b; Knoblauch et al., 2018; Lokshina et al., 2019; Walter Anthony et al., 2014). At a eutrophic fen site in Siberia, the higher CH_4 production than CO_2 production was attributed to proportions of CH_4 produced through acetoclastic (Equation 2) versus hydrogenotrophic (Equation 1) methanogenesis; adding an inhibitor to change the major pathway from acetoclastic to hydrogenotrophic methanogenesis increased CO_2:CH_4 ratios from 0.3-0.4 to 0.7-0.9 (Lokshina et al., 2019).

The notion that the CO_2:CH_4 production ratio can be less than 1:1 during anaerobic C mineralization is also supported by field measurements and modeling. Due to the diffusion of gases through meters of dense, silt-dominated sediments in yedoma lake taliks being prohibitively slow, yedoma talik sediments favor ebullition through secondary pore channels as a gas escape mechanism (Tan et al., 2015). ^{14}C-CH_4 measured in ebullition bubbles is older than ^{14}C-CO_2 from the same bubbles (Walter Anthony et al. 2018), suggesting that the CH_4 in ebullition bubbles comes from older, deeper sediment and the CO_2 comes from younger sediments closer to the sediment-water interface. The concept that CH_4 production dominates in deep taliks and that the dissolved gases giving rise to diffusive fluxes originate from surface lake sediments is further supported by ^{14}C-CH_4 ages of dissolved CH_4 being much younger than ^{14}C-CH_4 in ebullition bubbles (Elder et al., 2019). Ebullition bubbles released from deep with taliks are typically > 85% CH_4 and < 2% CO_2 (Walter et al. 2006; Walter Anthony et al., *submitted*), which may indicate that the CO_2:CH_4 production rates are skewed towards greater CH_4 than CO_2 production. In order for CH_4 to be produced in excess of CO_2, an inorganic source of H_2 is required. Telling et al. (2015) showed that pulverization of silicate rocks beneath glaciers produces abiogenic H_2; future research should explore the possibility that pulverization of rocks generating wind-blown silt could have also led to abiogenic H_2 in syngenetically aggraded yedoma permafrost sediments, enabling higher CH_4 production in deep yedoma talik sediments.

CO_2:CH_4 ratios of pore water dissolved gas measured in the Vault Lake core ranged from 1.2 to 10.7 (mean 4.6; Fig. 8; Winkel et al., 2019). The lowest CO_2:CH_4 ratio (1.2; 557 cm depth) was found at the thaw boundary, a region which also had higher relative abundance of the acetoclastic methanogens *Methanosaeta* (Winkel et al., 2019). These results would be consistent with the suggestion that acetoclastic methanogenesis leads to lower CO_2:CH_4 production ratios. However, the α_C values (an indicator of CH_4 production pathway; $\alpha_C > 1.06$ indicates CO_2 reduction; $\alpha_C < 1.04$ indicates acetate fermentation; Walter et al., 2008) in both the dissolved gas and ebullition bubbles indicate that CH_4 in the deepest part of the talik is produced primarily by CO_2 reduction (Fig. 8d). The α_C of dissolved gas in the pore water ranged from 1.044 to 1.087 (mean ± SD 1.066 ± 0.009; n = 38) and in bubbles released from the base of the talik in boreholes was 1.066 ± 0.005 (mean ± SE; n = 5); α_C in hotspot ebullition seeps, which are thought to be the deepest-seated naturally occurring ebullition seeps in taliks was 1.054 ± 0.006 (n = 5); and, α_C in ebullition seeps originating from shallower sediments was 1.048 ± 0.005 (n = 8).

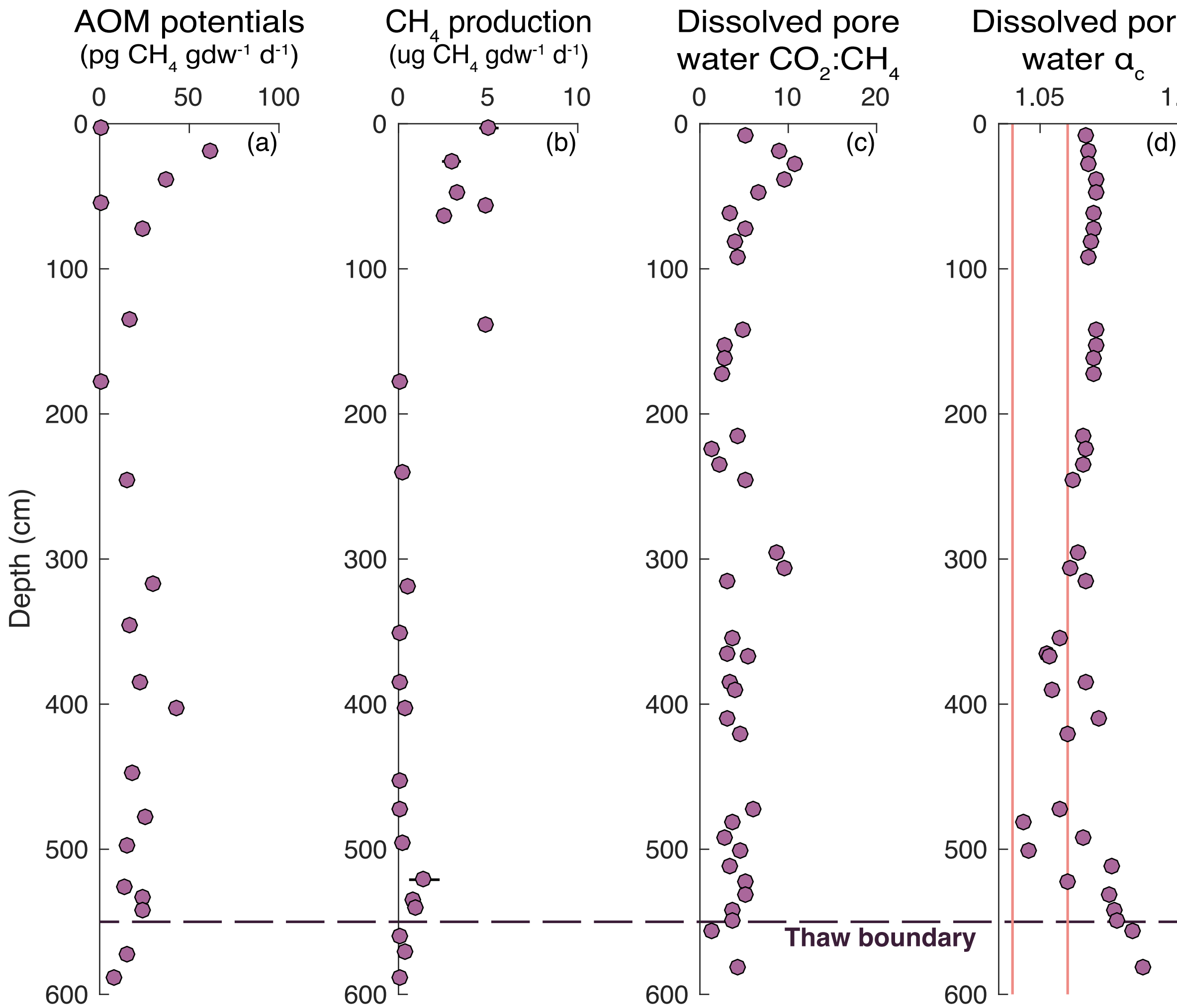

Figure 8. Magnitudes of AOM potentials (a; Winkel et al., 2019) and CH_4 production potentials (b; Heslop et al., 2015) measured in incubations of sediments from the Vault Lake core. Measurements of CO_2 and CH_4 concentrations in sediment pore waters from the Vault Lake core (Winkel et al., 2019) were used to calculate *in situ* CO_2:CH_4 ratios (c) and α_C (d).

. The highest CO_2:CH_4 ratios in porewater dissolved gases (8.6-10.7) were found in the surface organic rich mud (18-38 cm depth) and in the taberite (296-306 cm depth) facies. This is consistent with regions in the core found to have higher rates of AOM, which would decrease CH_4 concentrations and increase CO_2 concentrations. $\delta^{13}C$-CO_2 becomes increasingly depleted as CH_4 is oxidized to CO_2. Hence, enriched values of $\delta^{13}C$-CO_2 indicate very little CH_4 oxidation, while depleted values indicate more CH_4 oxidation. With the exception of one borehole bubble gas sample, in which $\delta^{13}C-CO_2$ was -20.7 ‰ and the corresponding $\delta^{13}C-CH_4$ was -66.2 ‰, borehole bubbles at Vault Lake had enriched ‰ values ($\delta^{13}C-CO_2$ -5.1 to -15.4 ‰; $\delta^{13}C-CH_4$ -74.2 to -75.5 ‰; Winkel et al., 2019). This indicates CH_4 produced at the base of the talik is subject to less AOM, which is supported by the low CO_2:CH_4 porewater ratios at this depth. In contrast, bubbles occurring from natural ebullition seeps draining free-phase gas from shallower sediments had more depleted $\delta^{13}C-CO_2$ (-14.0 to -26.2 ‰) and more enriched $\delta^{13}C-CH_4$ (-63.0 to -75.5 ‰), suggesting these bubbles were formed from pore space gas that was more influenced by AOM.

7. Potential changes with climate warming

Thermokarst lake formation alters local thermal dynamics, leading to lateral and vertical thaw and erosion, the formation of taliks (Brewer, 1958), and mobilization C previously sequestered in permafrost (Fig. 9). A process-based climate-sensitive lake biogeochemical model by Tan et al. (2015) indicated that seasonal variation in CH_4 emissions can be explained by energy input. In mesocosm warming experiments conducted in a shallow pond in the Netherlands, warming by 4 °C increased ebullitive CH_4 flux by 51%, but did not significantly affect diffusive CH_4 flux (Aben et al., 2017). The combination of increased energy input due to warmer temperatures and increased substrate potential due to additional permafrost thaw suggest additional climate warming will increase CH_4 fluxes and production in thermokarst lakes such as Vault Lake.

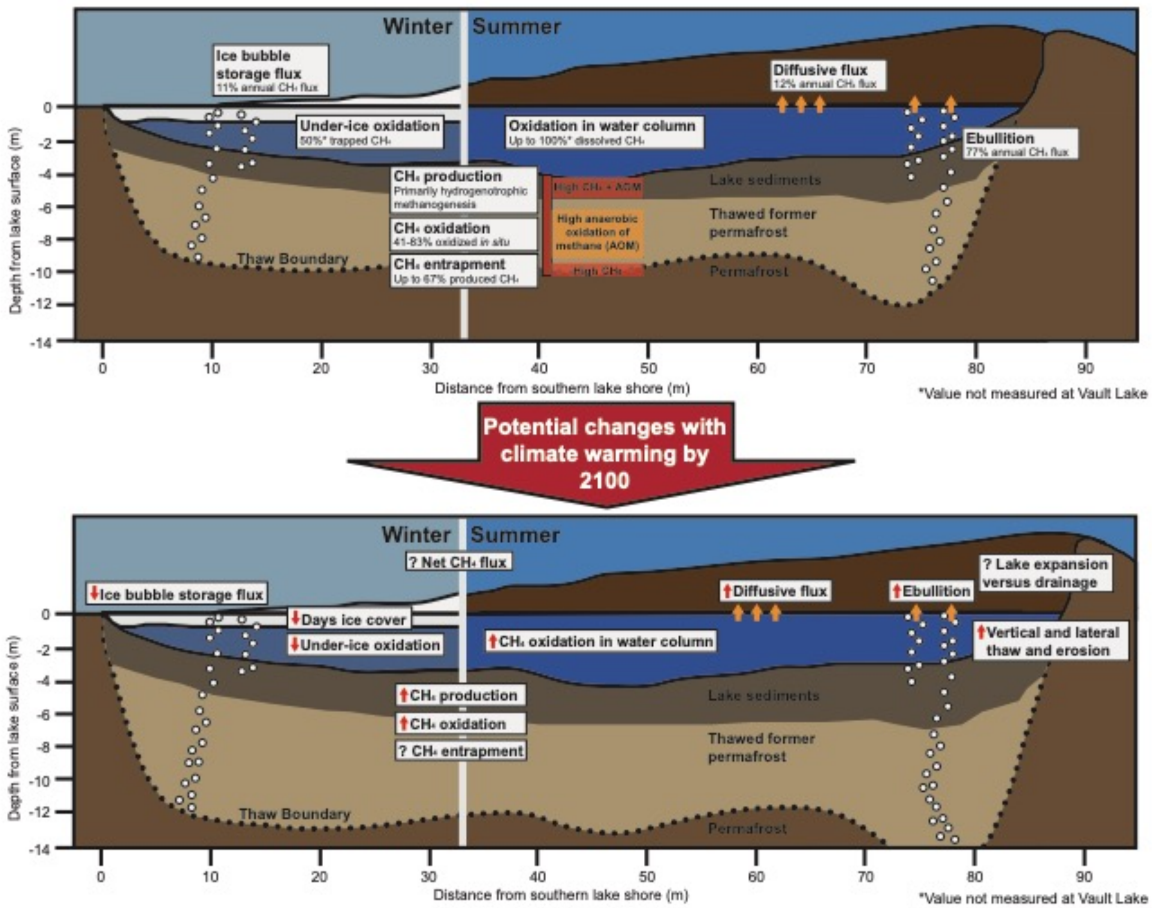

Figure 9. Current and future CH_4 dynamics in a thermokarst lake environment. Climate warming is expected to lead to increased lateral and vertical thaw and erosion, which may lead to lake expansion or lake drainage (see section 8 below). In addition, warmer temperatures are expected to lead to increased CH_4 production and oxidation and increased ebullitive and diffusive flux. Fewer days under ice cover are anticipated to reduce ice storage bubble flux and under-ice CH_4 oxidation. The net effects on annual CH_4 flux remain uncertain, although literature suggests these combined factors will lead to increases in CH_4 flux from thermokarst lakes with additional warming. See Section 8 for additional discussion of uncertainties.

Temperature sensitivity analyses conducted on sediments from the Vault Lake core suggest CH_4 production in recently-thawed former permafrost is highly sensitive to warming and thaw (0 °C to 3 °C; Heslop et al., 2019a). Therefore, we postulate permafrost warming and thaw at the base of the talik increases the available activation energy to initiate the chemical reactions involved in CH_4 production (Contant et al., 2011), and subsequently increases the number of methanogens and CH_4 production rates (Knoblauch et al., 2018, Wei et al., 2018). Acetoclastic methanogens, which were in higher relative abundance near the thaw front, have lower temperature optima than hydrogenotrophic methanogens (Allen et al., 2014) and therefore may be more suited to metabolic processes at these colder temperatures. While incubated sediments from near the thaw boundary had high temperature sensitivities at lower incubation temperatures, the sediments did not produce significantly more CH_4 at higher incubation temperatures (10 °C and 25 °C; Heslop et al., 2019a). This suggests current CH_4-producing microbial communities near the thaw boundary are not substrate-limited and optimized for colder temperatures.

While increased energy input from permafrost thaw increases CH_4 production at lower temperatures, at temperatures consistent with thermokarst lake taliks (4 °C) CH_4 production is only at 17% of maximum activity (Metje and Frenzel, 2007). Laboratory incubation studies suggest the optimal temperatures for methanogenesis are between 26-28 °C (Metje and Frenzel, 2007). This implies additional warming will cause a second increase in CH_4 production. In sediments of the Vault Lake core estimated to have been thawed centuries (100 to 400 years), CH_4 production did not significantly increase with warming at lower incubation temperatures (0 °C to 3 °C) but increased when sediments were warmed to temperatures above those observed *in situ* (10 °C and 25 °C; Heslop et al., 2019a). This implies that the former permafrost thawed for centuries, which currently has low CH_4 production potentials (Heslop et al., 2015; Kessler et al., 2012) due to low substrate bioavailability (Heslop et al., 2017) and/or the establishment of AOM microbial communities (Winkel et al., 2019), has the potential to support additional CH_4 production following additional warming. This increased CH_4 production potential may be due to increased substrate bioavailability due to higher ambient energy in warmer temperatures, a shift in microbial communities from predominately methanotrophs to predominately methanogens, or a combination thereof. In a landscape context, such additional warming of these sediments may occur with warmer atmospheric temperatures and/or further thermokarst or thermo-erosion exposing and mobilizing these sediments in the landscape.

While warming will increase CH_4 production rates in lake sediments, we expect the increased production may be partially offset by increased CH_4 consumption rates (Oh et al., 2020). However, in a nearby yedoma thermokarst lake in Interior Alaska, higher Q_{10} values for methanogenesis ($Q_{10} = 8.5 \pm 0.1$) versus aerobic CH_4 oxidation ($Q_{10} = 2.7 \pm 0.3$) in the water column suggest increases in CH_4 production will outpace increases in CH_4 consumption (Sepulveda-Jauregui et al., 2018). Further, it has been suggested that the shortening of ice cover periods in thermokarst lakes due to warming and increasing snow thickness (Arp et al. 2018) leads to more CH_4 being emitted into the atmosphere via direct ebullition instead of being oxidized while trapped under ice (Elder et al., 2019; Greene et al., 2014). In Finnish boreal lakes, more ice-free days have also been linked to greater diffusive CH_4 flux (Guo et al., 2020). Additional research is necessary to determine how these different controls will affect net CH_4 emissions with warming in thermokarst and northern lakes.

8. Future research directions

Thermokarst lake expansion versus drainage.

Ongoing efforts to constrain the diverse impacts of climate change and permafrost thaw on thermokarst lake expansion or drainage are critical for determining future CH_4 release potentials, as the landscape wetting (lake expansion) versus drying (lake drainage) will influence whether permafrost C is thawed under aerobic or anaerobic conditions (Lawrence et al., 2015). While in the Interior Alaska region near Vault Lake, net thermokarst lake area has increased by ~43% since 1949 (Walter Anthony et al., *submitted*), an examination of continental-scale Landsat imagery transects in North America and Eurasia found northern net lake area decreased 1.45% between 1999 and 2014 (Nitze et al., 2018). Despite net lake area decreases, thermokarst lake expansion by lateral shore erosion in Arctic-Boreal lowlands with ice-rich permafrost continues to cause significant gross lake area growth (transformation of land area to lake area; (Nitze et al., 2018). This in turn leads to growth of taliks and thawed sediment volumes under lakes (Walter Anthony et al., 2018). Mobilized permafrost C in taliks would be processed in anaerobic environments, meaning it is released as both CH_4 and CO_2. On the other hand, lake drainage changes local thermal dynamics such that: (1) taliks formed beneath a lake can refreeze and (2) near-surface C is more likely to be mineralized under aerobic conditions as CO_2.

Physical entrapment of CH_4.

Our first-order calculations suggest up to 99% of CH_4 produced at Vault Lake is not emitted into the atmosphere. Coupled with our estimates that 32-83% of produced CH_4 is oxidized *in situ* (Martinez-Cruz et al. 2017; Winkel et al., 2019), this suggests that 16-67% of produced CH_4 becomes entrapped within the Vault Lake system. While we acknowledge these values are rough first order estimates, they suggest periodic physical entrapment plays a substantial role in thermokarst lake CH_4 budgets. The location and fate of this entrapped CH_4 is not well constrained; however, rapid and sustained ebullition (for at least one day) observed in boreholes distributed across Vault Lake drilled in 2013 to map the talik dimensions suggests a large volume of gas was entrapped in sediments. Voids observed in freshly split sediment cores collected from thermokarst lakes, including Vault Lake (Heslop, *unpublished data* Walter Anthony, *unpublished data*), are suggestive of gas pockets storing CH_4 within the sediment. While to our knowledge these gas bubbles have not been quantified in thermokarst lake sediments, laboratory incubations examining gas bubble formation in wetland sediments suggest gas-filled voids, which are a precursor to the formation of ebullition bubble conduits, store more gas in clay and silt sediments (maximum 18.8% volumetric gas content) than sandy and silty sediments (maximum 13.2% and 12.0% volumetric gas content, respectively; Liu et al., 2016). In these laboratory incubations, hydrostatic head drop was linearly correlated with the magnitude of ebullition episodes releasing stored gas (Liu et al., 2016).

Depending on the phase and location of the entrapped gas, it may or may not be subject to CH_4 oxidation. Only the dissolved phase of CH_4 is subject to oxidation, so if gases are stored as bubbles in sediments, then the bubble phase protects CH_4 from *in situ* oxidation. For instance, the $\delta^{13}C$-CH_4 values of bubbles released from the borehole drilling at Vault Lake (mean -73‰, n = 5 samples) suggests that this trapped gas was not enriched by oxidation. Additional, high-resolution analyses in multiple thermokarst lakes to determine if and where entrapped CH_4 is subject to additional oxidation and what physical factors determine if and how it can be released will help better constrain the role of CH_4 emissions from thermokarst lakes in the PCF.

Incorporating thermokarst C dynamics into models

First-order models indicate up to 20% of the permafrost region is anticipated to experience physical disturbance thaw processes by 2300 (Turetsky et al., 2020), with GHG emissions from thermokarst lakes having the potential to more than double the PCF this century (Schneider von Deimling et al. 2015, Walter Anthony et al. 2018). Yet, large-scale global models predicting the magnitude of the PCF currently only consider gradual thaw processes (e.g. active layer deepening) and do not incorporate potential C emissions from rapid thaw processes, including thermokarst lakes (Turetsky et al., 2020). Improved understanding CH_4 dynamics within thermokarst lake environments will aid in incorporating their GHG emissions into future estimates of the PCF. While there have been studies modelling the formation of taliks beneath water bodies and subsequent potential C emissions under different climate scenarios (Kessler et al., 2012; Langer et al., 2016; Schneider von Deimling et al., 2015) and a process-based climate-sensitive lake biogeochemical model predicting CH_4 emissions (Tan et al., 2015), additional research is needed to incorporate these models into larger scale permafrost thaw and C dynamic models. Our work at Vault Lake suggests that the sediment layers of the talik experience different rates of methanogenesis and AOM due to varying substrate potentials and microbial communities, supporting the suggestion by Tan et al. (2015) that variability of CH_4 emissions can be primarily explained by energy input and substrate availability. In turn, this led to the facies experiencing different responses to additional warming. Integrating this depth-dependent variability in thermokarst lake GHG production dynamics into thermokarst models, including spatially dynamic estimates of CO_2:CH_4 production ratios, CH_4 oxidation, and gas release versus entrapment, is a first step in refining our estimates of how rapid thaw processes will contribute to the PCF. Given the variation we see between sediment layers within the same core at one thermokarst lake, it is necessary to examine additional thermokarst lake cores from diverse Arctic environments to determine how permafrost thaw history, sediment background, and OM and microbial characteristics influence CH_4 dynamics. Examining spatial variability within the same lake, including variation in facies thicknesses, talik depth, microbial communities, and substrate potential, will further refine estimates of potential GHG emissions from thermokarst lakes. More drilling studies capturing entire talik profiles are necessary to determine if patterns observed at Vault Lake hold true for other thermokarst lakes, including thermokarst lakes in non-yedoma regions.

In additional to additional field sampling to constrain variability, we suggest one approach to accounting for this spatial and temporal heterogeneity in models is to adopt a microscale approach, where variabilities in substrate availability, the microbiome, and energy are incorporated into geochemical rate models (e.g. Neumann et al., 2016) to predict CH_4 production and consumption rates in each facies. The predicted GHG production and consumption rates can then be integrated into whole-lake models that take into account thaw beneath lakes (e.g. Kessler et al., 2012; Langer et al., 2016; Schneider von Deimling et al., 2015), and eventually into larger models predicting the impact of thermokarst lakes on the PCF (e.g. Turetsky et al., 2020; Walter Anthony et al., 2018).

9. Summary and conclusions

At Vault Lake in Interior Alaska, a typical recently-formed thermokarst lake in a lowland permafrost setting with yedoma deposits, we observed depth-dependent variations in CH_4 production and oxidation. Variations in CH_4 production and oxidation potentials corresponded with changes in CO_2:CH_4 ratios and net CH_4 production response to temperature increases. The top 150 cm of the Vault Lake core had the highest CH_4 production potentials in 3 °C incubations, but oxidation potentials suggest 41-83% of the produced CH_4 is anaerobically oxidized *in situ*. This region also had higher CO_2:CH_4 ratios compared to the remainder of the core. The sediments near the thaw boundary, which prior modelling and ebullition bubble mapping studies of thermokarst lakes suggested are an important source of CH_4 production, had the highest *in situ* CH_4 concentrations and high CH_4 production potentials in incubations. CH_4 production near the thaw boundary was sensitive to warming at temperatures consistent with *in situ* temperatures in the talik and did not respond to additional warming. Further, the lowest CO_2:CH_4 ratio was observed near the thaw boundary, potentially due to higher proportions of CH_4 being produced through acetoclastic versus hydrogenotrophic methanogenesis. Former permafrost sediments, thawed centuries ago, had high CO_2:CH_4 ratios that were potentially influenced by high AOM rates. These sediments also experienced significant increases in net CH_4 production when warmed to temperatures above those observed *in situ*.

While not studied at Vault Lake, additional processes within the water column such as CH_4 oxidation and heterotrophic C respiration affect CO_2:CH_4 ratios and how much CH_4 is emitted into the atmosphere. The form of CH_4 in the thermokarst lake system (bubbles versus dissolved) is a key control on whether CH_4 is subject to *in situ* oxidation. Therefore, more research is necessary to better constrain how processes such as CH_4 storage within the system, including storage in sediments and under ice cover, affect lake CH_4 dynamics and emissions.

Acknowledgements

We thank: P. Anthony, S. Billings, N. Haubenstock, F. Horn, T. Howe, A. Saborowski, and B. Van Veldhuizen for assistance in data collection and/or analysis and S. Skidmore for granting access to Vault Lake. Funding for J.K. Heslop, K.M. Walter Anthony, A. Sepulveda-Jauregui, G. Grosse, and A. Bondurant was provided by DOE DE-SC0006920, NSF OPP-1107892, and ARC-1304823. Funding for K. Martinez-Cruz was provided by Conacyt 330197/233369. K.M. Walter Anthony was supported by NASA ABoVE NNX15AU49A. Additional funding for M. Winkel and K. M. Walter Anthony was provided by the NSF ARCSS-1500931 and for G. Grosse by ERC 388335. The Helmholtz Young Investigator Group of S. Liebner is funded by the Helmholtz Gemeinschaft (HGF) (VH-NG-919). Additional funding for J. Heslop was provided by a GFZ Discovery Fellowship. a UAF Center for Global Change Student Research Grant with funds from the UAF Center for Global Change, and STAR Fellowship Assistance agreement no. FP-91762901-0 awarded by the US Environmental Protection Agency (EPA). This manuscript has not been formally reviewed by EPA. The views expressed in this presentation are solely

those of J. Heslop, and the EPA does not endorse any products or commercial services mentioned.

References

Aben, R.C.H., Barros, N., van Donk, E. et al., 2017. Cross continental increase in methane ebullition under climate change. Nature Communications, 8, 1682.

Allen, D.T., Torres, V.M., Thomas, J., et al., 2013. Measurements of methane emissions at natural gas production sites in the United States. PNAS, 110 (44), 17768-17773.

Alvarez, R.A., Zavala-Araiza, D., Lyon, D.R., et al., 2018. Assessment of methane emissions from the U.S. oil and gas supply chain. Science, 361(6398), 186-188.

Arp, C.D., Jones, B.M., Liljedahl, A.K., et al., 2015. Depth, ice thickness, and ice-out timing cause divergent hydrologic responses among Arctic lakes. Water Resources Research, 51(12), 9379-9401.

Arp, C.D., Jones, B.M., Engram, M., et al., 2018. Contrasting lake ice responses to winter climate indicate future variability and trends on the Alaskan Arctic Coastal Plain. Environmental Research Letters, 13(12), 125001.

Bastviken, D., Tranvik, L.J., Downing, J.A., et al., 2011. Freshwater Methane Emissions Offset the Continental Carbon Sink. Science, 331(6013), 50-50.

Brewer, M.C., 1958. The thermal regime of an Arctic lake. Eos, 39(2), 278-284.

Brosius, L.S., Walter Anthony, K.M., Grosse, G., et al., 2012. Using the deuterium isotope composition of permafrost meltwater to constrain thermokarst lake contributions to atmospheric CH_4 during the last deglaciation. Journal of Geophysical Research, 117, G01022.

Cai, C., Leu, A.O., Xie, G.J., et al., 2018. A methanotrophic archaeon couples anaerobic oxidation of methane to Fe(III) reduction. ISME Journal, 12(8), 1929-1939.

Canfield, D.E., Kristensen, E., and Thamdrup, B., 2005. The Methane Cycle. Advances in Marine Biology, 48, 383-418.

Conant, R.T., Ryan, M.G., Ågren, G.I., et al., 2011. Temperature and soil organic matter decomposition rates- synthesis of current knowledge and a way forward. Global Change Biology, 17, 3392–3404.

Conrad, R., 1999. Contribution of hydrogen to methane production and control of hydrogen concentrations in methanogenic soils and sediments. FEMS Microbiology Ecology, 28, 193e202.

Coolin, M.J.L., and Orsi, W.D., 2015. The transcriptional response of microbial communities in thawing Alaskan permafrost soils. Frontiers in Microbiology, doi.org/10.3389/fmicb.2015.00197

Davidson, E.A., Janssens, I.A., 2006. Temperature sensitivity of soil carbon decomposition and feedbacks to climate change. Nature, 440, 165-173.

Dean, J.F., Meisel, O.H., Rosco, M.M., et al., 2020. East Siberian Arctic inland waters emit mostly contemporary carbon. Nature Communications, 11, 1627.

de Jong, A.E.E., In 't Zandt, M.H., Meisel, O.H., et al., 2018. Increases in temperature and nutrient availability positively affect methane-cycling microorganisms in Arctic thermokarst lake sediments. Environmental Microbiology, 20(12), 4314-4327.

Douglas, P.M.J, Moguel, R.G., Walter Anthony, K.M., et al., 2020. Clumped Isotopes Link Older Carbon Substrates With Slower Rates of Methanogenesis in Northern Lakes. Geophysical Research Letters, 47(6), e2019GL086756.

Drake, T.W., Wickland, K.P., Spencer, R.G.M., et al., 2015. Ancient low–molecular-weight organic acids in permafrost fuel rapid carbon dioxide production upon thaw. PNAS, 112(45), 13946-13951.

Elder, C.D, Xu, X., Walker, J., et al., 2018. Greenhouse gas emissions from diverse Arctic Alaskan lakes are dominated by young carbon. Nature Climate Change, 8(2), 166-171.

Elder, C.D., Schweiger, M., Lam, B., et al., 2019. Seasonal sources of whole-lake CH_4 and CO_2 emissions from Interior Alaskan thermokarst lakes. Journal of Geophysical Research: Biogeosciences, doi.org/10.1029/2018JG004735.

Engram, M., Walter Anthony, K.M., Scahs, T., et al., 2020. Remote sensing northern lake methane ebullition. Nature Climate Change, 10, 511–517.

Etminan, M., Myhre, G., Highwood, E.J., et al, 2016. Radiative forcing of carbon dioxide, methane, and nitrous oxide: A significant revision of the methane radiative forcing. Geophysical Research Letters, 43, 12,614– 12,623/

Ettwig, K.F., Butler, M.K., Le Paslier, D., et al., 2010. Nitrite-driven anaerobic methane oxidation by oxygenic bacteria. Nature, 464(7288), 543-548.

Ewing, S.A., O'Donnell, J.A., Aiken, G.R., et al., 2015. Long-term anoxia and release of ancient, labile carbon upon thaw of Pleistocene permafrost. Geophysical Research Letters, 42(24), 10,730-10,738.

Greene, S., Walter Anthony, K.M., Archer, D., et al., 2014. Modeling the impediment of methane ebullition bubbles by seasonal lake ice. Biogeosciences, 11, 6791–6811.

Günthel, M., Klawonn, I., Woodhouse, J., et al., 2020. Photosynthesis-driven methane production in oxic lake water as an important contributor to methane emission. Limnology & Oceanography, doi 10.1002/lno.11557

Guo, M., Zhuang, Q., Tan, Z., et al., 2020. Rising methane emissions from boreal lakes due to increasing ice-free days. Environmental Research Letters, doi 10.1088/1748-9326/ab8254.

Haroon, M.F., Hu, S., Shi, Y., et al., 2013. Anaerobic oxidation of methane coupled to nitrate reduction in a novel archaeal lineage. Nature, 500(7464), 567-70.

Heslop, JK, Walter Anthony, K.M., Sepulveda-Jauregui, A, et al., 2015. Thermokarst lake methanogenesis along a complete talik profile. Biogeosciences 12, 4317–4331.

Heslop, JK, Walter Anthony, K.M., Zhang, M., 2017. Utilizing pyrolysis GC-MS to characterize organic matter quality in relation to methane production in a thermokarst lake sediment core. Organic Geochemistry 103, 43-50.

Heslop JK, Walter Anthony KM, Grosse G, et al., 2019a. Century-scale time since permafrost thaw affects temperature sensitivity of net methane production in thermokarst-lake and talik sediments. Science of The Total Environment, 691, 124-134.

Heslop JK, Winkel M, Walter Anthony KM, et al., 2019b. Increasing organic carbon biolability with depth in yedoma permafrost: ramifications for future climate change. Journal of Geophysical Research: Biogeosciences, 124(7), 2021-2038.

Huttunen, J.T., Alm, J., Liikanen, A., et al., 2003. Fluxes of methane, carbon dioxide and nitrous oxide in boreal lakes and potential anthropogenic effects on the aquatic greenhouse gas emissions. Chemosphere, 52, 609–621.

Ionescu, D., Bizic-Ionescu, M., Khalili, A. et al., 2015. A new tool for long-term studies of POM-bacteria interactions: overcoming the century-old Bottle Effect. Scientific Reports, 5, 14706.

Jansen, E., Christensen, J.H., Dokken, T., et al., 2020. Past perspectives on the present era of abrupt Arctic climate change. Nature Climate Change https://doi.org/10.1038/s41558-020-0860-7

Jones, B.M., Grosse, G., Arp, C.D., et al., 2011. Modern thermokarst lake dynamics in the continuous permafrost zone, northern Seward Peninsula, Alaska. Journal of Geophysical Research: Biogeosciences, 116, G00M03.

Jorgenson, M.T., Yoshikawa, K., Kanevskiy, M., et al., 2008. Permafrost characteristics of Alaska. In: Kane, D., Hinkel, K. (Eds.), Proceedings of the Ninth International Conference on Permafrost. University of Alaska, Fairbanks, AK, pp. 121-122.

Kessler, M.A., Plug, L.J., and Walter Anthony, K.M., 2012. Simulating the decadal- to millennial-scale dynamics of morphology and sequestered carbon mobilization of two thermokarst lakes in NW Alaska. Journal of Geophysical Research: Biogeosciences, 117, G00M06.

Knittel, K., and Boetius, A., 2009. Anaerobic Oxidation of Methane: Progress with an Unknown Process. Annu. Rev. Microbiol., 63, 311–334.

Knoblauch, C., Beer, C., Liebner, S., et al., 2018. Methane production as key to the greenhouse gas budget of thawing permafrost. Nature Climate Change, 8, 309–312.

Kuhn, MK, Lundin, EJ, Giesler, R, et al., 2018. Emissions from thaw ponds largely offset the carbon sink of northern permafrost wetlands. Scientific Reports 8, 9535.

Langer, M., Westermann, S., Boike, J., et al., 2016. Rapid degradation of permafrost underneath waterbodies in tundra landscapes—Toward a representation of thermokarst in land surface models. Journal of Geophysical Research: Earth Surface, 121(12), 2446-2470.

Lawrence, D.M., Koven, C.D, Swenson, S.C., et al., 2015. Permafrost thaw and resulting soil moisture changes regulate projected high-latitude CO_2 and CH_4 emissions. Environmental Research Letters.,10, 094011.

Lindgren, P.R., Grosse, G., Walter Anthony, K.M., and Meyer, F.J., 2016. Detection and spatiotemporal analysis of methane ebullition on thermokarst lake ice using high-resolution optical aerial imagery. Biogeosciences, 13, 27–44.

Lindgren, P.R., Grosse, G., Meyer, F.J., and Walter Anthony, K.M., 2019. An Object-Based Classification Method to Detect Methane Ebullition Bubbles in Early Winter Lake Ice. Remote Sensing, 11(7), 822.

Liu, F., Kou, D., Abbott, B.W., et al., 2019. Disentangling the Effects of Climate, Vegetation, Soil and Related Substrate Properties on the Biodegradability of Permafrost-Derived Dissolved Organic Carbon. Journal of Geophysical Research: Biogeosciences, 124(11), 3377-3389.

Liu, L., Wilkinson, J., Koca, K., et al., 2016. The role of sediment structure in gas bubble storage and release. Journal of Geophysical Research: Biogeosciences, 121, 1992–2005.

Lokshina, L., Vavilin, V., Litti, Y., et al., 2019. Methane Production in a West Siberian Eutrophic Fen Is Much Higher than Carbon Dioxide Production: Incubation of Peat Samples, Stoichiometry, Stable Isotope Dynamics, Modeling. Water Resources, 46, S110–S125.

Matthews, E., Johnson, M.S., Genovese, V., et al., 2020. Methane emission from high latitude lakes: methane-centric lake classification and satellite-driven annual cycle of emissions. Scientific Reports, 10, 12465.

Martinez-Cruz, K, Sepulveda-Jauregui, A, Walter Anthony, KM., et al., 2015. Geographic and seasonal variation of dissolved methane and aerobic methane oxidation in Alaskan lakes. Biogeosciences 12, 4213–4243.

Martinez-Cruz, K., Leewis, M.-C., Herriott, I.C., et al., 2017. Anaerobic oxidation of methane by aerobic methanotrophs in sub-Arctic lake sediments. Science of the Total Environment, 607-608, 23–31.

Martinez-Cruz, K, Sepulveda-Jauregui, A, Casper, P., et al., 2018. Ubiquitous and significant anaerobic oxidation of methane in freshwater lake sediments. Water Research, 144. 332e340.

Metje, M., and Frenzel, P., 2007. Methanogenesis and methanogenic pathways in a peat from subarctic permafrost. Environmental Microbiology, 9(4), 954-64.

Nitze, I., Grosse, G., Jones, B.M., et al., 2018. Remote sensing quantifies widespread abundance of permafrost region disturbances across the Arctic and Subarctic. Nature Communications, 9, 5423.

Oh, Y., Zhuang, Q., Liu, L. et al., 2020. Reduced net methane emissions due to microbial methane oxidation in a warmer Arctic. Nature Climate. Change 10, 317–321.

Olefeldt, D., Goswami, Grosse, G., et al., 2016. Circumpolar distribution and carbon storage of thermokarst landscapes. Nature Communications, 7, 13043.

Osudar, R., Liebner, S., Alawi, M., et al., 2016. Methane turnover and methanotrophic communities in arctic aquatic ecosystems of the Lena Delta, Northeast Siberia. FEMS Microbiology Ecology, 92(8), fiw116.

Oswald, K., Milucka, J., Brand, A., et al., 2016. Aerobic gammaproteobacterial methanotrophs mitigate methane emissions from oxic and anoxic lake waters. Limnology and Oceanography, 61(S1), S101-S118.

Parsekian, A.D., Grosse, G., Walbrecker, J.O., et al., 2013. Detecting unfrozen sediments below thermokarst lakes with surface nuclear magnetic resonance. Geophysical Research Letters, 40, 535-540.

Post, E., Alley, R.B., Christensen, T.R., et al, 2019. The polar regions in a 2°C warmer world, Science Advances, 5(12), eaaw9883.

Reeburgh, W.R., 2007. Oceanic Methane Biogeochemistry. Chem. Rev., 107, 486−513.

Repo, E., Huttunen, J.T., Naumov, A.V., et al., 2007. Release of CO_2 and CH_4 from small wetland lakes in western Siberia. Tellus B: Chemical and Physical Meteorology, 59(5), 788-796.

Scandella, B.P., Varadharajan, C., Hemond, H.F., et al., 2011. A conduit dilation model of methane venting from lake sediments, Geophysical Research Letters, 38, L06408.

Schädel, C., Schuur, E., Bracho, R., et al., 2014. Circumpolar assessment of permafrost C quality and its vulnerability over time using long-term incubation data. Global Change Biology, 20, 641–652.

Schirrmeister, L., Meyer, H., Andreev, A., et al., 2016. Late Quaternary paleoenvironmental records from the Chatanika River valley near Fairbanks (Alaska). Quaternary Science Reviews, 147, 259-278.

Schneider von Deimling, T., Grosse, G., Strauss, J., et al., 2015. Observation-based modelling of permafrost carbon fluxes with accounting for deep carbon deposits and thermokarst activity, Biogeosciences, 12, 3469–3488.

Schuur, E., McGuire, A., Schädel, C., 2015. Climate change and the permafrost carbon feedback. Nature 520, 171–9.

Selvam, B.P., Lapierre, J.-F., Guillemette, F., et al., 2017. Degradation potentials of dissolved organic carbon (DOC) from thawed permafrost peat. Scientific Reports 7, 45811.

Sepulveda-Jauregui, A., Walter Anthony, K.M., Martinez-Cruz, K., et al., 2015. Methane and carbon dioxide emissions from 40 lakes along a north south latitudinal transect in Alaska. Biogeosciences 12, 3197–3223.

Sepulveda-Jauregui, A., Hoyos-Santillan, J., Martinez-Cruz, K., et al., 2018. Eutrophication exacerbates the impact of climate warming on lake methane emission. Science of The Total Environment, 636, 411-419.

Smith, L.C., Sheng, Y., and MacDonald, G.M., 2007. A First Pan-Arctic Assessment of the Influence of Glaciation, Permafrost, Topography and Peatlands on Northern Hemisphere Lake Distribution, Permafrost and Periglacial. Processes, 18, 201–208.

Spangenberg, I., Overduin, P.P., Damm, E., et al., 2020. Methane Pathways in Winter Ice of Thermokarst Lakes, Lagoons and Coastal Waters in North Siberia. The Cryosphere Discuss., in review.

Tan, Z., Zhuang, Q., and Walter Anthony, K.M., 2015. Modeling methane emissions from arctic lakes: model development and site-level study, J. Adv. Model. Earth Sy. 07, doi:10.1002/2014MS000344.

Tan, Z., Zhuang, Q., Shurpali, N.J., et al., 2017. Modeling CO_2 emissions from Arctic lakes: Model development and site-level study, J. Adv. Model. Earth Sy. 09, 2190-2213.

Tanski, G., Wagner, D., Knoblauch, C., et al., 2019. Rapid CO_2 Release From Eroding Permafrost in Seawater. Geophysical Research Letters 46, 11244–11252.

Telling, J., Boyd, E.S., Bone, N., et al., 2015. Rock comminution as a source of hydrogen for subglacial ecosystems. Nature Geoscience, 8, 851-855.

Thalasso, F., Sepulveda-Jauregui, A., Gandois, L., et al., 2020. Sub-oxycline methane oxidation can fully uptake CH_4 produced in sediments: case study of a lake in Siberia. Scientific Reports, 10, 3423.

Tveit, A.T., Urich, T., Frenzel, P., and Svenning, M.M., 2015. Metabolic and trophic interactions modulate methane production by Arctic peat microbiota in response to warming. PNAS, 112(19), E2507-E2516.

Turetsky, MR, Abbott, BW, Jones, MC, Anthony, KW, 2019. Permafrost collapse is accelerating carbon release. Nature 569, 32-34.

Turetsky, M.R., Abbott, B.W., Jones, M.C. et al., 2020. Carbon release through abrupt permafrost thaw. Nature Geoscience, 13, 138–143.

Varadharajan, C., 2009. Magnitude and spatio-temporal variability of methane emissions from a eutrophic freshwater lake. Ph.D. dissertation, Mass. Inst. of Technol., Cambridge.

Voigt, C., Marushchak, M.E., Abbott, B.W., et al., 2020. Nitrous oxide emissions from permafrost-affected soils. Nature Reviews Earth and Environment, 1, 420–434.

Vonk, J. E., Tank, S. E., Mann, P. J., et al., 2015. Biodegradability of dissolved organic carbon in permafrost soils and aquatic systems: a meta-analysis, Biogeosciences, 12, 6915–6930.

Walter, Zimov, Chanton, et al., 2006. Methane bubbling from Siberian thaw lakes as a positive feedback to climate warming. Nature 443, 71–75.

Walter, K.M., Chanton, J.P., Chapin III, F.S., et al., 2008. Methane production and bubble emissions from arctic lakes: Isotopic implications for source pathways and ages. Journal of Geophysical Research: Biogeosciences, 113, G00A08.

Walter Anthony, K.M., Vas, D.A., Brosius, L., et al., 2010. Estimating methane emissions from northern lakes using ice- bubble surveys. Limnol. Oceanogr. Methods, 8, 592–609.

Walter Anthony, K.M., Anthony, P., Grosse, G., and Chanton, J., 2012. Geologic methane seeps along boundaries of arctic permafrost thaw and melting glaciers. Nature Geoscience, 5, 419–426.

Walter Anthony, KM, Zimov, SA, Grosse, G, et al., 2014. A shift of thermokarst lakes from carbon sources to sinks during the Holocene epoch. Nature 511, 452–456.

Walter Anthony, K.M., Daanen, R., Anthony, P., et al., 2016. Methane emissions proportional to permafrost carbon thawed in Arctic lakes since the 1950s. Nature Geoscience, 9, 679-681.

Walter Anthony, K., Schneider von Deimling, T., Nitze, I. et al., 2018. 21st-century modeled permafrost carbon emissions accelerated by abrupt thaw beneath lakes. Nature Communications, 9, 3262.

Walter Anthony, K.M., Lindgren, P., Hanke, P., et al., *submitted*. Decadal-scale hotspot CH_4 emission following abrupt permafrost thaw. Environmental Research Letters.

Wei, S., Cui, H., Zhu, Y., et al., 2018. Shifts of methanogenic communities in response to permafrost thaw results in rising methane emissions and soil property changes. Extremophiles, 22, 447–459.

Weyhenmeyer, G., Kosten, S., Wallin, M. et al., 2015. Significant fraction of CO_2 emissions from boreal lakes derived from hydrologic inorganic carbon inputs. Nature Geoscience, 8, 933–936.

Wik, M., Varner, R., Anthony, K. et al., 2016. Climate-sensitive northern lakes and ponds are critical components of methane release. Nature Geoscience, 9, 99–105.

Williams, P. J. and Smith, M. W., 1989. The Frozen Earth: Fundamentals of Geocryology, Cambridge University Press, Cambridge, UK.

Winkel, M., Sepulveda-Jauregui, A., Martinez-Cruz, K., et al., 2019. First evidence for cold-adapted anaerobic oxidation of methane in deep sediments of thermokarst lakes. Environmental Research Communications, 1, 2.

Zimov, S.A., Voropaev, Y.V., Semiletov, I.P., et al., 1997. North Siberian Lakes: A Methane Source Fueled by Pleistocene Carbon. Science, 277(5327), 800-802.